MASTER OF SCIENCE

Investigating the role of transcription factor Nrf2 in the pathogenesis of NAFLD

Wood, K. L.

Award date:
2017

Investigating the role of transcription factor Nrf2 in the pathogenesis of NAFLD

KL Wood

Supervised by Professor John F Dillon and Professor John D Hayes

Masters by Research

May 2017

University of Dundee

Table of Contents

List of Illustrations

List of Tables

List of Abbreviations

Acaa	Acetyl-CoA Acyltransferase 1
Acc1	Acetyl-CoA carboxylase
Acox1	Acyl-CoA Oxidase 1
ACS	Acyl-CoA synthetase
ALD	Alcoholic liver disease
ALT	Alanine aminotransferase
AMP	Adenosine monophosphate
AMPK	AMP-activated protein kinase
ARE	Antioxidant response element
AST	Aspartate aminotransferase
Atf	Activating transcription factor
ATP	Adenosine triphosphate
B220	Protein tyrosine phosphatase receptor type C (PTPRC)
Bip	Binding immunoglobulin protein
C/ebp	CAAT/enhancer binding protein
Ces1	Carboxylesterase 1
Chop	CAAT/enhancer binding protein (C/EBP) homologous protein
Chrebp	Carbohydrate responsive element–binding protein
CO_2	Carbon dioxide
CoA	Co-enzyme A
Cpt-1	Carnitine palmitoyl transferase 1
Cpt-2	Carnitine palmitoyl transferase 2
Creb	Cre-binding protein
DMSO	Dimethyl sulfoxide
DNA	Deoxyribonucleic acid
Dnajb11	DnaJ Heat Shock Protein Family (Hsp40) Member B11
Dnajb9	DnaJ Heat Shock Protein Family (Hsp40) Member B9
DPP-4	Dipeptidyl peptidase 4
Edem	ER Degradation Enhancing Alpha-Mannosidase Like Protein 1
Eif2α	Eukaryotic initiation factor 2 α
EpRE	Electrophile response element
ER	Endoplasmic reticulum
ERAD	ER associated degradation
Ero1α	Endoplasmic reticulum oxidoreductin 1α
F4/80	EGF-like module-containing mucin-like hormone receptor-like 1 (EMR1)
Fabp	Fatty acid binding protein
FAD	Flavin adenine dinucleotide
Fasn	Fatty acid synthase
Fat/Cd36	Fatty acid translocase
Fatp	Fatty acid transport protein
Fgf-21	Fibroblast growth factor 21
Foxo1	Forkhead box protein 1
FXR	Farnesoid X receptor
Gadd34	Growth arrest and DNA damage-inducible protein
Gcl	Glutamate-Cysteine Ligase

Gclc	Glutamate-Cysteine Ligase Catalytic Subunit
Gclm	Glutamate-Cysteine Ligase Modifier Subunit
GLP-1	Glucagon-like peptide-1
Gpat	Glycerol-3-phosphate acyltransferases
Gpx	Glutathione peroxidase
Grp94	Glucose regulated protein (Endoplasmin)
GSH	Glutathione
Gsk3	Glycogen synthase kinase 3
Gsr	Glutathione Disulfide Reductase
GSSG	Glutathione disulphide
Gst	Glutathione S-transferase
HCC	Hepatocellular carcinoma
HFFr	High fat high fructose
Hmox1	Haem-oxygenase 1
HSC	Hepatic stellate cells
Il6	Interleukin 6
Ire1	Inositol-requiring enzyme 1
Jnk	Jun-amino-terminal kinase
Keap1	Kelch like-ECH-associated protein 1
LDL	Low density lipoprotein
LPS	Lipopolysaccharide
LXRα	Liver X receptor α
MDA	Malondialdehyde
Mpo	Myeloperoxidase
mRNA	Messenger ribonucleic acid
Mttp	Microsomal triglyceride transfer protein
NADPH	Reduced nicotinamide adenine dinucleotide phosphate
NAFLD	Non-alcoholic fatty liver disease
NAS	NAFLD activity score
NASH	Non-alcoholic steatohepatitis
NC	Normal chow
Nos2	Nitric oxide synthase 2
Nqo1	NAD(P)H quinone dehydrogenase 1
Nrf2	Nuclear receptor (erythroid-derived 2)-like 2
p38 Mapk	p38 mitogen-activated protein kinase
$p58^{IPK}$	DnaJ heat shock protein family (Hsp40) member C3
Pdi	Protein disulfide isomerase
PdiA3	Protein disulfide-isomerase A3
PdiA4	Protein disulfide-isomerase A4
Perk	Protein kinase RNA-like endoplasmic reticulum kinase
Pparα	Peroxisome proliferated activating receptor α
Pparγ	Peroxisome proliferated activating receptor γ
Pparγc1	Peroxisome proliferated activating receptor γ – coactivator 1
PPRE	Peroxisome proliferator response element
PUFA	Polyunsaturated fatty acids
REDOX	Reduction–oxidation

RER	Rough endoplasmic reticulum
RIDD	Regulated Ire1α dependent decay
ROS	Reactive oxygen species
rtPCR	Reverse transcriptase polymerase chain reaction
Rxr	Retinoid X receptor
Scd1	Stearoyl-CoA desaturase 1
SCF/βTrCP	Skp1-Cul1-F-box ubiquitin ligase
SER	Smooth endoplasmic reticulum
Serp1	Stress Associated Endoplasmic Reticulum Protein 1
SFA	Saturated fatty acids
SOD	Superoxide dismutase
SRE	Sterol regulatory element
Srebp-1a	Sterol regulatory element–binding protein 1a
Srebp-1c	Sterol regulatory element–binding protein 1c
Stc2	Stanniocalcin 2
TBE-31	Tricyclic bis(cyano enone)
TG	Triacylglycerides
TIIDM	Type II diabetes mellitus
Tnf	Tumour necrosis factor
Tnfα	Tumour necrosis factor
TPARS	Thiobarbituric acid- reactive substances
Traf	TNF Receptor Associated Factor
TUNEL	Terminal deoxynucleotidyl transferase (TdT) dUTP Nick-End Labeling
UPR	Unfolded protein response
VLDL	Very low density lipoprotein
WT	Wild type
Xbp1	X-box binding protein 1
Xbp1-s	X-box binding protein 1 - spliced
Xbp1-u	X-box binding protein 1 - unspliced

Acknowledgements

I would like to thank my supervisors Professor John F Dillon and Professor John D Hayes for allowing me the opportunity to undertake this Masters project. A huge thank you to the team in the Hayes lab, in particular my laboratory supervisor Dr Ritu Sharma for all her advice and Mrs Kimimuepigha Ebisine for support with practical skills. I would also like to thank the Melville Trust for funding a summer vacation project in 2015 that introduced me to this field. Finally, many thanks to family and friends for support (and proofreading!)

Declaration

I declare that I am the author of this thesis and that this work has not previously been submitted for a higher degree. I confirm that I have performed the work reported within and that all references cited within this thesis have been consulted unless otherwise stated.

Kayleigh Wood

Abstract

The pathogenesis of non-alcoholic steatohepatitis (NASH) is thought to occur through interacting mechanisms of cellular stress. Lipids accumulate within hepatocytes, making cells more susceptible to insult and less able to respond to challenges, leading to progression from simple steatosis to inflammation.

Endoplasmic reticulum (ER) stress occurs when mis-folded proteins accumulate in the ER lumen and cellular requirement exceeds the capacity of the ER to modify proteins. ER stress activates pathways that act to attenuate stress or prompt apoptosis if ER homeostasis cannot be achieved. The transcription factor nuclear receptor (erythroid-derived 2)-like 2 (Nrf2) is a master regulator that orchestrates the response to oxidative stress by inducing expression of cytoprotective genes. Understanding interactions between oxidative and ER stress may allow further understanding of the pathogenesis of NASH.

The role of Nrf2 in response to ER stress was investigated using mouse epithelial fibroblasts, comparing WT to $Nrf2^{-/-}$ and cells with increased Nrf2 activity. ER stress was induced and expression of ER stress response proteins was analyzed.

Results demonstrate that $Nrf2^{-/-}$ cells have increased expression of ER stress response proteins under basal conditions compared to WT. The response to ER stress also varied with cellular Nrf2 status: Maximal response to glucose deprivation occurred at 4 hours in both WT and $Nrf2^{-/-}$ cells, but occurred at 6hours in cells with increased Nrf2 availability. The magnitude of the response was smaller in $Nrf2^{-/-}$ cells, suggesting that $Nrf2^{-/-}$ cells have less ability to respond to ER stress. It is proposed that Nrf2 is involved in a negative feedback mechanism, whereby increased Nrf2 activity helps to alleviate ER stress and subsequently down-regulates the ER response.

Chapter 1 Introduction

1.1 NON-ALCOHOLIC FATTY LIVER DISEASE (NAFLD)

1.1.1 Overview

Non-alcoholic fatty liver disease (NAFLD) is a condition characterised by the accumulation of lipids within hepatocytes. NAFLD encompasses a spectrum of histopathological severity, ranging from simple steatosis to increasing levels of inflammation, known as non-alcoholic steatohepatitis (NASH), which can occur with or without fibrosis (1).

Historically, NASH was thought to be related to undisclosed alcohol intake because of the histological similarities with alcoholic liver disease (ALD) (2). However, the development of fatty liver in confirmed non-drinkers, particularly associated with obesity, type II diabetes mellitus (TIIDM) and hyperlipidaemia was increasingly recognised (2). The term NASH was first used to characterise this distinct condition in the 1980s by Ludwig et al. in a classical case series of 20 patients with documented histopathological findings (3). Since this time NAFLD and NASH have become widely accepted and are generally considered to be the hepatic manifestations of obesity and metabolic dysfunction.

1.1.2 The natural history of NAFLD

1.1.2.1 Associations and epidemiology

NAFLD is frequently associated with a sedentary lifestyle, calorific excess and visceral adiposity; it is therefore unsurprising that alongside trends in obesity, NAFLD is becoming increasingly common (1, 4, 5). An increase in the fructose component in the western diet has been postulated as a possible cause of the increasing prevalence of this condition (6). NAFLD is now considered to be the most common cause of chronic liver disease, with a global prevalence of approximately 25% (1). The proportion of patients with NAFLD who have NASH varies between populations, ranging from 6-29%; however this reaches almost 60% in cases where biopsy is clinically indicated (7). NASH has become the second leading cause of liver transplantation in the United States (7).

1.1.2.2 Disease progression and complications

A significant proportion of NAFLD patients develop progressive liver disease, which in the most severe cases can result in fibrosis, cirrhosis and end stage liver failure (1). NASH, and fibrosis in particular, is also associated with the development of hepatocellular carcinoma (HCC) (1). The natural history of NAFLD often follows a gradual process of increasing severity, however the NAFLD population is heterogeneous and a subgroup of patients experiences a more rapid deterioration (1). Simple steatosis has typically more benign outcomes, however, up to 4% of patients still develop cirrhosis within a 20-year period (1). Patients with NASH characteristically have more aggressive disease, with an increased risk of complications and more rapid development of cirrhosis (1).

There are many factors that influence disease progression, including individual variation, genetic and environmental factors and comorbid disease. NAFLD can occur as part of the metabolic syndrome, a multisystem disorder of metabolic derangement and excess comprising obesity, hypertension, dyslipidaemia and insulin resistance. TIIDM is a risk factor for more severe disease, and male patients with co-existing metabolic syndrome are at an increased risk of HCC development (1).

1.1.2.3 Population health impact

Despite the fact that only a small proportion of patients develop severe complications of NAFLD, the high prevalence of disease within the population creates a significant public health burden. Patients with NAFLD frequently have comorbid metabolic disease and NASH is associated with an increased cardiovascular morbidity and mortality (7). Therefore many patients have multiple health issues and a significant proportion may progress to serious complications including, but not limited to, end stage liver disease.

Due to the increasing burden of obesity associated liver disease, delineation of the biochemical pathways underlying the pathophysiology and disease progression of steatosis to NASH is of great importance. Insight into this area could aid identification of new, more accurate diagnostic methods and

understanding key molecular events may allow the development of targeted drug treatments. Although it is likely that multiple factors contribute to NAFLD, establishing the mechanism of liver injury is also key to allow prevention strategies.

1.1.3 Current Management of Patients with NAFLD

1.1.3.1 Clinical Presentation and diagnosis

NAFLD can be asymptomatic, and is often discovered incidentally following abnormalities in routine biochemistry (2, 8). Symptomatic patients may present with right upper quadrant pain, or nonspecific complaints such as fatigue (2, 8). Investigations typically demonstrate mild to moderate increases in serum transaminases, alanine aminotransferase (ALT) and aspartate aminotransferase (AST), which are nonspecific indicators of hepatocyte damage, and findings of increased hepatic echogenicity on ultrasound scan supports steatosis. Diagnosis of NAFLD is clinical, after the exclusion of other potential aetiologies including autoimmune, drug related, ALD and viral hepatitis. Diagnosis of NASH requires histological evidence of inflammation, in the presence of steatosis without other causes of liver disease (8).

1.1.3.2 Liver biopsy and histopathological features

Liver biopsy for histological assessment is considered to be the gold standard for diagnosis of NASH, however this is associated with small but significant mortality risk, and is therefore performed only in cases when clinically necessary, or for research purposes (8). NAFLD is histologically defined as the presence of visible lipid droplets in >5% of hepatocytes and features of NASH include fatty changes, lobular inflammation, Mallory-Denk bodies, fibrosis and necrosis (9). The NAFLD activity score (NAS) is a frequently used research tool to score histological severity of disease (10).

1.1.3.3 Follow up and management

Management of fatty liver primarily involves lifestyle modifications of diet and exercise to facilitate weight loss, with major improvements typically occurring with >10% weight loss (8, 11, 12). There are a number of scoring tools that can be used to stratify patients and identify those most at risk of disease progression

and fibrosis; these include the Enhanced Liver Fibrosis Score, NAFLD fibrosis score, Fibrosis-4 index and AST to platelet ratio (8, 11). There are currently no targeted treatments for NAFLD, however some studies have demonstrated modest improvements in histological features and serum enzymes with vitamin E and peroxisome proliferated activating receptor γ (PPARγ) agonists such as pioglitazone (11). In the UK, guidelines recommend these treatments be considered in patients with advanced fibrosis (8). Research into potential treatments is on going and includes therapies used in managements of TIIDM such as glucagon-like peptide-1 (GLP-1) receptor agonists, dipeptidyl peptidase 4 (DPP-4) inhibitors as well as CC-chemokine receptor antagonists and farnesoid X receptor (FXR) agonists (11, 12). Evidence from the FLINT trial, a multicentre, randomised placebo-controlled clinical trial in 283 NASH patients demonstrated that obeticholic acid, a synthetic bile acid and FXR agonist significantly improved histological features compared to placebo, with the main reported adverse effect of pruritus (13). Although this result seems promising, further evidence on efficacy, benefits and safety is required (13).

1.1.4 Current hypotheses of pathology in NAFLD

There has been much interest in characterising the key pathways underpinning the development of NAFL and NASH, reviewed in (14). NAFLD is a heterogeneous condition, with genetic and environmental factors further influencing an individual's susceptibility to disease development and progression (12). The predominant theory of pathogenesis is the multiple hit model, whereby insulin resistance and hepatic storage of triacylglycerides is compounded by further cellular insult, leading to inflammation and fibrosis (15, 16). Areas under study include the inflammatory response, intestinal microbiome, adipose tissue dysfunction, mitochondrial dysfunction, nutritional factors and the role of insulin resistance (17).

The initial accumulation of fat in hepatocytes results from an imbalance in lipid homeostasis alongside adipose tissue inflammation and dysfunction(14). Steatotic hepatocytes are more vulnerable to damage, and cellular dysfunction can be exacerbated by further insults such as direct lipotoxicity, oxidative stress, endoplasmic reticulum (ER) stress, and mitochondrial dysfunction (14).

Damaged and apoptotic hepatocytes release cellular components. These, along with proinflammatory cytokines (e.g. tumour necrosis factor α (Tnfα)), adipokines and bacterial endotoxins, activate resident hepatic macrophages, Kupffer cells (14). This results in further cytokine and chemokine release, recruitment of monocytes and amplification of the proinflammatory response (14). The components that induce inflammation can also prime and activate hepatic stellate cells (HSC), which transdifferentiate to a myofibroblast phenotype, promoting collagen production and fibrosis (14). The following sections will provide more detail on the molecular pathways[1] involved in lipid homeostasis, oxidative stress and ER stress.

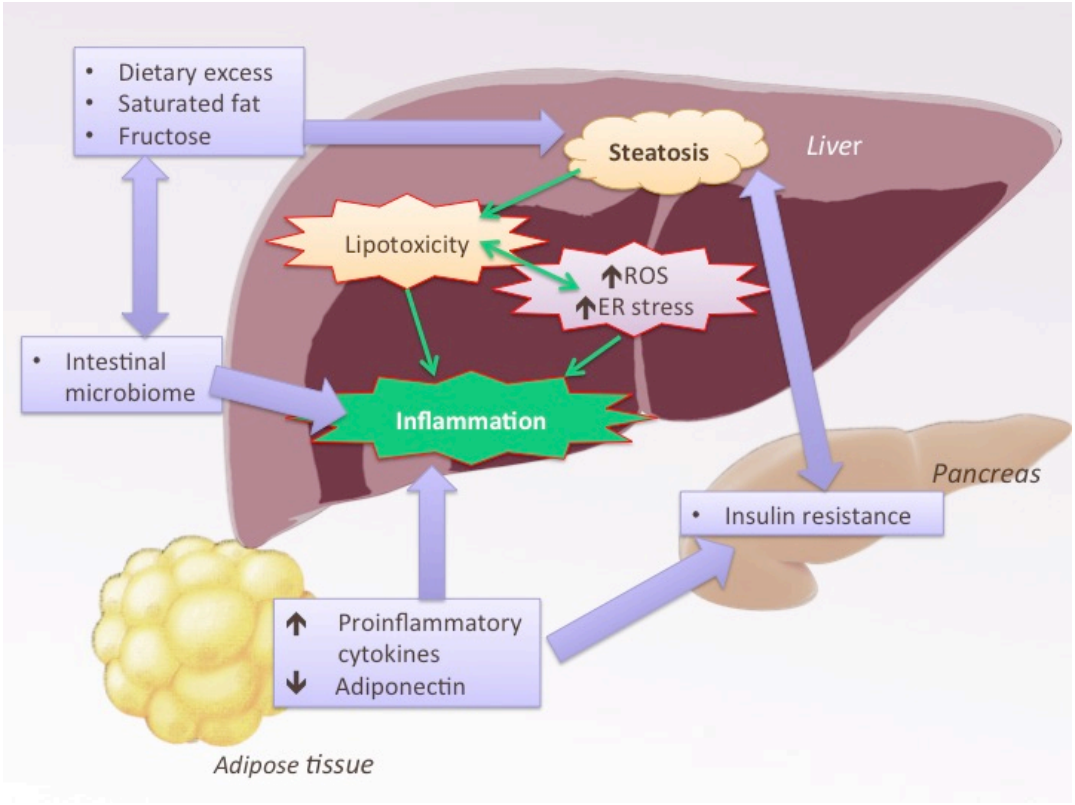

Figure 1.1 Mechanisms potentially contributing to the pathogenesis of fatty liver disease, adapted from (15)

[1] For clarity, because this project has utilised mouse tissues and a murine cell line, pathways will be described using standard murine gene/protein abbreviations, unless discussing specific studies in human tissues.

1.2 LIPID PATHWAYS

Energy homeostasis relies on the balance of intake and expenditure: Calorific excess results in an anabolic state promoting synthesis and storage, for example the storage of fatty acids as triglycerides in adipose tissue. In contrast, nutrient deprivation results in a catabolic state promoting the mobilisation and metabolism of energy stores to provide substrates for adenosine triphosphate (ATP) production. The liver, endocrine pancreas and adipose tissue are highly involved in regulating the response to metabolic status, which relies on coordinated interactions and responses between these organs.

1.2.1 Lipid homeostasis in the liver

The liver is the primary site of lipid processing and esterification, and lipid homeostasis is perturbed in NAFLD. Lipid input is derived from three main sources: Dietary intake in the form of chylomicrons, free fatty acids mobilised and released from existing adipose stores, and fatty acids newly synthesised from carbohydrates during *de novo* lipogenesis (14, 18). Lipid output occurs through export, for example into plasma as lipoproteins, incorporation into cellular components and metabolism via beta-oxidation (18). Uptake of circulating free fatty acids into hepatocytes is proportional to serum concentration and occurs through passive diffusion or facilitated transport by fatty acid transport protein (Fatp) and fatty acid translocase (Fat/Cd36) (18). After entering the cell, fatty acids bind to fatty acid binding protein (Fabp) or to acyl-Co-enzyme A (acyl-CoA) via acyl-CoA synthetase (Acs) enzymes, the latter producing fatty-acyl-CoA (18). These bound forms are then processed depending on the nutritional and energy status of the cell (18).

In states of positive energy balance, lipogenic pathways are activated. These involve the esterification of free fatty acids into more complex lipids including triacylglycerides (TG), phospholipids and lipoproteins (18). TGs comprise the common storage form of fatty acids, phospholipids are an integral component of cell membranes and lipoproteins have numerous and varied functions. Central enzymes involved in lipid biosynthesis and esterification include fatty acid

synthase (Fasn) and glycerol-3-phosphate acyltransferases (Gpat)s (18). Fasn also activates phospholipid synthesis in the ER (18).

The liver converts excess dietary carbohydrates into fatty acids in a process known as *de novo* lipogenesis (14). *De novo* lipogenesis comprises a series of cytosolic condensation reactions with the sequential addition of acetyl groups catalysed by acetyl-CoA carboxylase (Acc1). In this way, a starting molecule (such as acetyl-CoA) is converted into malonyl-CoA, which can then undergo further elongation and esterification; Acc1 is the rate-limiting enzyme in this process (18).

Under conditions of negative energy balance, fatty acids can be metabolised and utilised as a substrate for ATP generation through mitochondrial and peroxisomal beta-oxidation (18). Fatty acid transport across the outer and inner mitochondrial membranes is facilitated by the carnitine palmitoyl transferases, Cpt-1 and Cpt-2, respectively (19). Fatty-acyl-CoA undergoes initial dehydrogenation, donating electrons to cofactors that are then transferred to the electron transport chain (18). In beta-oxidation, 2 carbon units are consecutively removed from fatty-acyl-CoA, resulting in either complete oxidation to acetyl-CoA and CO_2, or incomplete oxidation producing ketone bodies (19). Acetyl-CoA can then be further metabolized in the citric acid cycle.

1.2.2 Transcriptional regulation of lipid homeostasis

Energy homeostasis is controlled at a transcriptional level by a coordinated group of metabolic regulators. These include members of the sterol regulatory element–binding protein family (e.g. Srebp-1a, Srebp-1c), peroxisome proliferator activated receptors (Pparα, Pparγ), adenosine monophosphate (AMP)-activated protein kinase (Ampk), Pparγ-coactivator 1 (Pparγc1), liver X receptor-like receptors (Lxrα, Fxr), CAAT/enhancer binding proteins (C/ebp), carbohydrate responsive element–binding protein family (Chrebp) and forkhead box protein 1 (Foxo1) (17, 18, 20). The following section will provide an overview of these regulatory pathways, with particular attention to lipogenesis and lipid degradation.

Three Srebp isoforms (Srebp-1a, -1c and Srebp-2) are involved in regulating lipogenic pathways; these are produced as inactive precursors bound to the ER membrane (20). When cellular levels of cholesterol are low, Srebp is escorted to the Golgi apparatus where it undergoes cleavage, releasing the active NH_2-terminal domain from the ER membrane (20). This active domain subsequently translocates to the nucleus and induces the expression of numerous target genes via the sterol regulatory element (SRE) DNA binding domain (20). Srebp target genes act to increase synthesis of fatty acids, triglycerides and cholesterol; significant lipogenic targets include Fasn, Acc1, ATP-citrate lyase (responsible for production of acetyl-CoA), Gpat and components of the fatty acid elongase complex (18, 20). Srebp also induces genes involved in production of NADPH (reduced nicotinamide adenine dinucleotide phosphate) which is a cofactor required for a number of biosynthetic reactions (20).

The Ppar family are ligand activated nuclear receptors that heterodimerise with retinoid X receptors (Rxrs) (21). When activated by ligands and alongside co-regulatory complexes, the heterodimer binds to the peroxisome proliferator response element (PPRE) DNA segment and regulates numerous metabolic genes (21). The Ppar family proteins have active sensory sites and are activated by endogenous ligands, which may include fatty acids and fatty acid derivatives(19, 22). Pparα is the most highly expressed Ppar isoform in the liver, and the principal role is to mobilise and degrade fatty acids through increased fatty acid oxidation (18). Pparα upregulates target genes that mobilise fatty acids, including Cpt-1, Cpt-2, Fabp and Fat/Cd36 (18, 19, 21). Pparα increases catabolism and acts to inhibit fatty acid biosynthetic pathways through the induction of malonyl-CoA decarboxylase, responsible for degradation of the fatty acid precursor malonyl-CoA(19). Interestingly, Pparα may be preferentially activated by *de novo* and dietary derived ligands, rather than fatty acids mobilised from adipose tissue (19), although this remains unclear (22). Pparα also participates in apoprotein production and lipoprotein assembly (18, 19, 21).

Pparγ is primarily expressed in adipose tissue; it is involved in adipocyte differentiation and acts to increase the expression of lipogenic enzymes including Fasn, Acc1, Fat/Cd36, Gpat and Fatp (18, 19). Pparγ expression in the liver is believed to mediate metabolic coordination between hepatic and adipose tissue (19).

Ampk is activated by an increasing ratio of AMP to ATP, allowing detection of cellular energy status (18). When activated, Ampk stimulates numerous metabolic pathways to increase cellular energy including fatty acid oxidation and represses synthetic pathways, by down regulating Acc1 (18).

Lxrα is a master regulator of cellular cholesterol flux, inducing genes involved in bile acid synthesis and excretion and dietary cholesterol absorption (18). Lxrα also transcriptionally regulates Srebp-1c; sterols activate Lxrα which in turn induces Srebp-1c and promotes fatty acid synthesis (18). Lxrα activation is competitively blocked by the presence of unsaturated fatty acids, therefore reducing Srebp-1c transcription; unsaturated fatty acids also accelerate the degradation of Srebp-1c mRNA (20). Bile salts re-entering via the enterohepatic circulation in the fed state act as ligands to activate FXRs (22). Activated Fxr appears to suppress lipogenesis, possibly by indirectly inhibiting Srebp-1c action (22). Evidence suggests that Fxr down-regulates Pparα target genes and may reduce fatty acid oxidation, however it also may induce lipolytic hormones including fibroblast growth factor 21 (Fgf-21) (22). This paradox suggests that Fxr may act in a modulatory capacity, differentially fine-tuning metabolic responses in fed and fasted states. Ppars, Lxrs and Fxrs all act as heterodimers with Rxrs, therefore it is likely that competitive antagonism for Rxr binding is involved in maintaining coordinated and non-contradictory responses to cellular lipid homeostasis (18). Energy homeostasis is also under hormonal control and is strongly influenced by the actions of hormones, insulin and glucagon secreted by the endocrine pancreatic, as well as by adipokines leptin and adiponectin from adipose tissue.

A simplified overview of regulatory lipid homeostasis pathways is given in Figure 1.2. A number of these regulators have been investigated as pharmacological targets for the treatment of metabolic disorders including dyslipidaemias, TIIDM and NASH. Ppar agonists include fibrate drugs acting on Pparα, used to treat hyperlipidaemias and thiazolidinediones that act on Pparγ are used in both TIIDM and NASH with fibrosis. As described in Section 1.1.4 above, Fxrs are potential therapeutic targets in NASH.

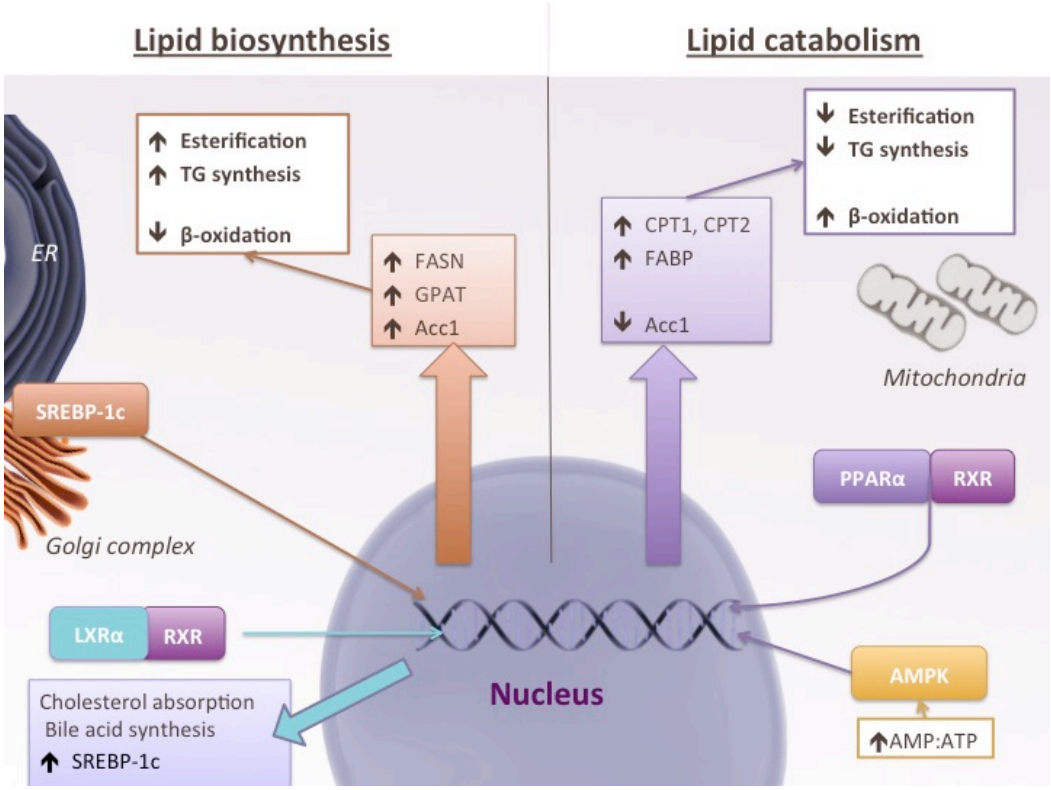

Figure 1.2 Overview of regulation of lipid homeostasis pathways

1.3 OXIDATIVE STRESS

1.3.1 Reactive oxygen species and cellular REDOX status

Oxidative stress is described as the damage and stress response resulting from an imbalance favouring oxidation in the cellular reduction-oxidation (REDOX) status (23, 24). The reactive oxygen species (ROS) superoxide anions ($O_2\bullet^-$), hydrogen peroxide (H_2O_2) and hydroxyl radicals (HO•) can be endogenously produced during physiological reactions or be derived from exogenous sources (23). These molecules have the potential to induce irreversible damage through oxidation of cellular components including proteins, lipids and nucleic acids. However, ROS are also vital in the immune defence against pathogens and are involved in REDOX signalling pathways promoting cellular adaptation (23).

The effects of ROS are variable depending on the amount and type of ROS produced as well as the subcellular localisation (23). Partial reduction of oxygen during aerobic respiration can generate superoxide, which undergoes rapid conversion to H_2O_2 by superoxide dismutase (SOD) enzymes (23). H_2O_2 is a less toxic ROS than superoxide and can be an important signalling molecule through regulated and reversible oxidation of cysteine thiol residues, induce conformational and functional protein alterations (23). Conversely, hydroxyl radicals are non-selective and toxic; mechanisms controlling iron homeostasis are particularly important to minimise the formation of these, which can be generated through the oxidation of ferrous ions (Fe^2) (23).

Oxidative stress can induce damage in numerous ways: Un-selective protein thiol oxidation can induce changes in protein structure and loss of function, lipid peroxidation can reduce the stability of phospholipid membranes, nucleic acid damage can introduce genomic instability and uncontrolled mitochondrial ROS can disrupt the respiratory chain (23, 24). Oxidative stress has been the focus of research in numerous conditions such as normal ageing, cardiovascular disease, diabetes and NASH, (reviewed in (17, 25, 26)).

Cells have developed numerous mechanisms to maintain REDOX homeostasis and adapt to oxidative challenge. These form a network of detoxifying enzymatic pathways and small antioxidant molecules that act in concert to neutralise or eliminate ROS. Many components involved in the cellular response to endogenous and exogenous oxidative stress are controlled at a transcriptional level by the Nrf2/ARE pathway described in Section 1.4.

1.3.2 Glutathione pathway

An important component of the cellular response to ROS is glutathione (GSH), an intracellular tripeptide composed of glutamyl, cysteinyl and glycine residues, with an active thiol group (24). GSH is involved in three general mechanisms of cellular antioxidant response: GSH can act directly as an electron donor; GSH can undergo conjugation with oxidised products and elimination; and GSH is a cofactor for antioxidant enzymes (24). In its capacity as a direct antioxidant, GSH reacts with ROS, reactive nitrogen species or electrophiles, and is converted to the oxidised form glutathione disulphide (GSSG) as shown in Equation 1 (24).

1) **R**OOH + 2GSH → ROH + GSSG + H_2O

The REDOX potential of a cell is often estimated from the ratio of GSH:GSSG (24). This depends on dynamic factors such as ROS generation and the balance between GSH production, consumption, recycling and elimination (24). GSH is produced in a two-stage process; the first step is peptide bond formation between glutamate and cysteine (24). This is catalysed by the enzyme glutamate-cysteine ligase (Glc) and is the rate-limiting step in biosynthesis (24). GSSG can be restored to GSH by the enzyme glutathione reductase (Gsr) with the cofactor NADPH, as shown in Equation 2 (24).

2) GSSG + NADPH + H^+ → 2GSH + $NADP^+$

GSH is synthesised in the cytosol and then distributed and maintained in relatively discrete pools in the cytosol, mitochondria, ER and nuclear compartments where it has organelle-specific functions (24). There has been

much interest in the mitochondrial GSH pool due to production of ROS associated with mitochondrial respiration. The role of GSH and GSSG in the ER is discussed further in Section1.5.

GSH is a cofactor in reactions catalysed by the glutathione peroxidase (Gpx) family of enzymes that reduce H_2O_2 and organic peroxides of free-fatty acids, cholesterols and phospholipids (24). Conjugation of GSH to electrophilic compounds is facilitated by a number of glutathione S-transferase (Gst) isoforms. The GSH-conjugate products are typically excreted or partially recycled (24).

1.4 NUCLEAR RECEPTOR (ERYTHROID-DERIVED 2)-LIKE 2 (NRF2)

1.4.1 The Nrf2/Antioxidant Response Element pathway

Nuclear receptor (erythroid-derived 2)-like 2 Nrf2 belongs to the Cap'n'Collar, basic leucine zipper family of transcription factors (27). Nrf2 is a master regulator that orchestrates the intracellular response to oxidative stress as well as activating transcription of over 250 genes targets, involved in diverse cellular functions including cytoprotection, antioxidant response, detoxification, and lipid and carbohydrate metabolism (27).

The common DNA binding region known as the antioxidant response element (ARE) (also known as the electrophile response element (EpRE)) was identified and characterised by Rushmore and colleagues in a series of studies in the early 1990s(28-30). The ARE is a highly conserved, cis-acting DNA motif found in the promoter region of many genes, including phase II metabolism enzymes (31). Itoh et al examined Nrf2 as a possible candidate to bind the ARE motif after identifying consensus sequence similarity (31). Through the generation of Nrf2-null mice, the study found that Nrf2 acts as an obligatory heterodimer with small-Maf proteins and is able to bind numerous ARE promoter sequences, demonstrating a common mechanism of phase II enzyme induction (31).

In association with regulatory cofactors, the Nrf2/sMaf heterodimer is able to induce the transcription of numerous target genes via the ARE promoter region. Canonical genes regulated by Nrf2 include major detoxification enzymes NAD(P)H quinone dehydrogenase 1 (Nqo1) and haem-oxygenase 1 (Hmox1), as well enzymes involved in the glutathione pathway, including the modifier (Gclm) and catalytic (Gclc) subunits of Gcl (the rate-limiting enzyme in glutathione synthesis) (27).

1.4.2 Nrf2-Keap1 association

Nrf2 is constitutively expressed; under basal conditions, it is sequestered in the cytoplasmic compartment in association with Kelch like-ECH-associated protein 1 (Keap1) via two binding sites in the Nrf2 Neh2 domain (32). Keap1 is a cysteine rich dimeric substrate adaptor protein that both anchors Nrf2 and

interacts with a cullin-3 RINGbox1 E3 ubiquitin ligase complex (27). This facilitates the continuous polyubiquitination and proteasomal degradation of Nrf2 by the Keap1-Cullin3-E3 ubiquitin ligase complex, maintaining Nrf2 at low levels (27).

Keap1 has many reactive cysteine residues, which induce a conformational change in the presence of oxidative and electrophilic species, allowing cells to sense alterations in intracellular redox status and respond to a variety of stimuli. The exact mechanism is not yet completely understood; early theories involve a hinge-and-latch mechanism, whereby ROS induce a conformational change in Keap1 resulting in the release of Nrf2 (33). However, recent evidence suggests that ROS activation of Keap1 leads to strengthened Nrf2 binding but a reduced ability of Keap1 to interact with the degradation complex (27). Thus, Keap1 would remain bound to non-degraded Nrf2 and newly synthesised Nrf2 would circumvent sequestration and degradation (27). Therefore, under conditions of oxidative stress Nrf2 is able to translocate to the nucleus, heterodimerise in complex with small maf proteins and activate transcription through the ARE.

Nrf2 is also under a further post-translational regulation through an independent mechanism involving glycogen synthase kinase 3 (Gsk-3) and the Skp1-Cul1-F-box ubiquitin ligase (SCF/βTrCP) complex (34). Gsk-3 phosphorylates residues within the Neh6 domain of Nrf2, enhancing association of βTrCP and promoting SCF/βTrCP dependent degradation (34).

1.4.3 Nrf2 in health and disease

There has been much research into Nrf2, as Nrf2 may confer a cellular survival advantage against oxidative insult that can be physiologically adaptive in normal cells. Due to this cellular protective role, suppression or ineffective Nrf2 could be a factor in inflammatory conditions resulting in cellular damage. However, constitutive activation, whether by Keap1 deletion or Nrf2 amplification, can also promote survival in pathological cells and up-regulation has been observed in a number of cancer lines (35). Uninhibited Nrf2 activity in tumour cells via loss of Keap1 can promote resistance to ROS inducing chemotherapeutic agents

(35). There is therefore a delicate balance between cellular survival, protection and tumorigenesis. Although it is known that Nrf2 has a key role in cellular defence against oxidative stress, the role of Nrf2 in different environments of cellular stress has not been fully explored. Nrf2 may be of particular importance in NAFLD: Nrf2 knockdown mice are known to be more susceptible to NASH (36, 37) and there is evidence demonstrating activation of the Nrf2/ARE pathway in the human disease, discussed further below.

1.4.4 Nrf2 in human NAFLD

Hardwick et al (2010) investigated the expression and activity levels of selected proteins induced by NRF2 in a total of 54 human liver samples (38). The tissue was scored using the NAS, histologically evaluated and categorised according to disease severity: Normal (n=20), steatotic (n=12), NASH and fatty (n=11) and NASH not fatty (n=11). Steatosis was determined by fatty infiltration of >10%, NASH (fatty) was categorised by the presence of macrovesicular fatty deposits and inflammation, and NASH (not fatty) samples demonstrated more severe inflammation and fatty infiltration of <5%.

GSH and TBARS (thiobarbituric acid- reactive substances) assays were used to assess cellular oxidative stress: Concentrations of GSH and GSSG as well as the GSH:GSSG ratio were found to be significantly decreased with progressive disease severity (38). TBARS assay demonstrated that malondialdehyde (MDA), produced by lipid peroxidation, also significantly increased with disease progression. This provides direct evidence that hepatocytes are subject to oxidative stress and lipid peroxidation in human NAFLD (38).

The expression and activity levels of NQO1, GST and GCL were assessed using a range of real-time, reverse transcriptase polymerase chain reaction (rtPCR), immunoblotting and enzyme activity assays. Results showed that NQO1 mRNA and relative cytosolic protein levels significantly increased with severity and progression of NAFLD (38). Furthermore, NQO1 enzymatic activity also increased with disease progression. GCLM mRNA showed an increasing trend but did not reach significance, and protein levels were unchanged. The mRNA expression of GST isoforms (A1, A2, A4, M3 and P1), and protein levels of GST

A and GST P were increased with disease progression. The enzymatic activity of GST showed decreasing activity with disease severity, which persisted even in the presence of supplemented GSH levels (38).

The study stained liver samples for NRF2 and the percentage nuclear translocation was averaged for each group: Immunohistochemistry demonstrated an average NRF2 nuclear translocation of ~2% of hepatocytes in normal liver samples (38). This was increased in the NAFLD groups, with nuclear translocation in an average of 25%, 23% and 22% of hepatocytes for steatotic, NASH (fatty) and NASH (not fatty) groups, respectively (38).

Taken together, these results demonstrate increasing levels of lipid peroxidation and oxidative stress as disease severity increases, alongside the nuclear translocation of NRF2 and induction of classical gene targets, NQO1 and GST. Although mRNA levels of certain GST isoforms were increased other isoforms (M1, M2 and M4) were not significantly different, and GST M protein levels were reduced. The authors suggest differential regulation of GST isoforms, and postulate that increased expression of GST P may indicate predisposition to fibrosis and HCC, noting that further study is required (38).

1.5 ENDOPLASMIC RETICULUM STRESS

1.5.1 The function of the endoplasmic reticulum (ER)

The endoplasmic reticulum (ER) is a specialised membranous organelle that extends from the outer nuclear membrane; it is subdivided functionally and structurally into the nuclear envelope, rough (RER) and smooth (SER) domains (39, 40). The RER and SER can be distinguished morphologically through association of the RER with ribosomal units, but also more importantly, by differences in membrane protein composition (39). Functions of the ER include the post-translational modification of newly synthesised proteins, detoxification and the biosynthesis of phospholipids and steroids (39, 40). Cells that have high levels of protein production, such as plasma cells that produce and secrete immunoglobulins have abundant ER. The ER lumen also comprises the major intracellular site of calcium storage, and the ER (and the specialised sarcoplasmic reticulum in myocytes) is highly involved in calcium homeostasis (39, 41).

1.5.1.1 Protein folding

Nascent proteins are released from ribosomes and transported across the ER membrane into the ER lumen. These mature as they traverse along the ER, undergoing modifications including folding, glycosylation, formation of tertiary protein structure and multiple subunit assembly (41). Mature proteins exit the ER and those destined for secretion or insertion into the plasma membrane are packaged in the Golgi apparatus (11).

1.5.1.2 ER REDOX status

Protein folding requires oxidation and disulphide bond formation so the ER lumen has a specialised REDOX environment to enable this (24, 42). Disulphide bond formation is catalysed by ER resident proteins, including protein disulphide isomerise (Pdi) and endoplasmic reticulum oxidoreductin 1α (Ero1α): Polypeptide chains are oxidised by Pdi, which subsequently undergoes oxidation by Ero1α in the presence of the co-substrate FAD (flavin adenine dinucleotide) (42). Ero1α re-enters this cycle following oxidation by molecular O_2 (42). The ER maintains a more oxidised environment than other subcellular compartments

as demonstrated by the GSH:GSSG ratio; in the ER the proportion of the oxidised form reaches up to 25% of total, compared to the cytosol where it typically comprises less than 1% (24).

1.5.1.3 Lipid and steroid biosynthesis

The ER is works in close concert with the Golgi complex and together these comprise the endomembranous compartment and are major sites of phospholipid synthesis (40). Phospholipids are integral cell membrane components and the most abundant of these are synthesised in the ER and Golgi organelles. Many enzymes involved in lipid biosynthetic pathways are associated with the ER, including acyltransferases such as Gpat (40), and lipid components of lipoproteins are also synthesised in the ER(18).

1.5.2 ER stress and the unfolded protein response (UPR)

Protein folding is a complex process in which errors can arise; cells have highly conserved mechanisms for the detection and resolution of such errors (41, 43-45). ER resident proteins are involved in pathways that maintain ER homeostasis, balancing the ER processing capacity to accommodate cellular protein requirements (41, 43-45). ER stress occurs when the capacity of the ER is overwhelmed, misfolded and unfolded proteins accumulate and the normal trafficking of proteins through the ER is disrupted (41, 43-45). ER stress stimulates an adaptive signalling network known as the unfolded protein response (UPR), which has been reviewed extensively (41, 43-46). Complimentary signalling pathways of the UPR act in concert to increase the capacity of the ER, reduce protein demand, and increase degradation of misfolded products (41, 43-45).

The UPR acts at a transcriptional level to down-regulate non-essential proteins while preferentially inducing cell survival proteins and upregulating ER chaperones and enzymes (41, 43-45). The UPR increases ER associated degradation (ERAD), stimulates phospholipid synthesis to lengthen the ER membrane (40) and slows the trafficking of proteins through the ER (43). The UPR is an adaptive mechanism that acts to attenuate and resolve ER stress,

however if homeostasis cannot be restored and chronic ER stress persists, the UPR ultimately activates proapoptotic pathways (41, 43).

1.5.3 Pathways of the UPR

The UPR is classically described as three complimentary signalling pathways, each of these relating to one of three proximal ER stress sensing transmembrane proteins; Inositol-requiring enzyme 1 (Ire1), protein kinase RNA-like endoplasmic reticulum kinase (Perk) and activating transcription factor 6 (Atf6) (41, 43-45). An overview of these pathways is described below and then depicted in Figure 1.3. Under non-stressed conditions, the ER chaperone binding immunoglobulin protein (Bip) moderates the activity of these proteins by binding to the luminal sensory domain, maintaining an inactive state (47). When unfolded proteins accumulate, Bip dissociates, promoting further signal transduction. This mechanism allows for a regulated, adaptive response to evolving conditions within the ER environment (47).

1.5.3.1 Ire1α and Xbp1

The transmembrane serine/threonine protein kinase Ire1 was the first identified ER stress sensor; initially discovered by Nikawa and Yamashita (48), the role of this protein in response to ER stress was characterised in yeast by Cox and colleagues in the Walter lab (49). The mammalian homologue, Ire1α, is ubiquitously expressed, particularly in the pancreas, and is preferentially localised to the nuclear membrane (50).

The N-terminal domain of Ire1α in the ER lumen detects perturbations in protein folding with fragments of unfolded polypeptide chains acting as ligands to activate Ire1 (42, 51, 52). Bip modulates activity by associating with Ire1α and reducing sensitivity in low ER stress environments, and also contributes to deactivation following by associating with Ire1α following the attenuation of ER stress (42).

Under conditions of ER stress, Ire1α undergoes oligomerization and trans-autophosphorylation of serine residues, resulting in the activation of a cytoplasmic endoribonuclease domain (53-55). Activated Ire1α has RNase

activity and directly cleaves an intron from the mRNA of X-box binding protein 1 (Xbp1) through an unconventional splicing mechanism, independently of the spliceosome; this is phylogenetically conserved between the mammalian Xbp1 and yeast homologue (Hac1) (53, 56, 57). Splicing of Xbp1 by Ire1α removes a 26-nucleotide intron, causing frameshift and the production of a larger and more stable protein, Xbp1-spliced (Xbp1-s) (53). There is some evidence that induction of Ire1α downstream targets requires cooperative activation of the Atf6 branch of the UPR to provide newly transcribed mRNA of Xbp1-unspliced (Xbp1-u) (53), however this has not been definitively proven (58).

The nuclease activity of Ire1α also increases the degradation of mRNAs in response to ER stress, possibly through direct cleavage (59). This reduces ER input in a process known as regulated Ire1α dependent decay (RIDD) (59).

The product Xbp1-s is a Cre-binding protein/Activating transcription factor (Creb/Atf) that translocates to the nucleus and induces the expression of UPR target genes such as components of ERAD machinery and ER chaperones, through the promoter UPR element (53, 58). Some evidence suggests that Xbp1-s specific targets include the DnaJ-like accessory proteins Dnajb9, Dnajb11 and $p58^{IPK}$, that act to augment chaperone activities, and Edem (ER degradation enhancing α-mannosidase-like protein), which participates in ERAD (58). Xbp1-s also has some autoregulatory activity and potentially cross-regulates Atf6 (58).

Xbp1 is essential for hepatocyte growth; the knockout of this gene is embryonically lethal in mice due to hepatic hypoplasia (60). Xbp1-s also induces the expression of many non-UPR target genes such as α-fetoprotein and α1-antitrypsin (60). Other targets are involved in lipid and glucose metabolism (61). For example, Xbp1-s is able to induce lipogenic genes independently of Srebp-1c, and in the fasted state upregulates the expression of Pparα (61).

1.5.3.2 Perk and Eif2α

Perk is another transmembrane kinase that undergoes oligomerization and trans-autophosphorylation: Phosphorylated (phospho)-Perk has kinase activity that

subsequently phosphorylates eukaryotic initiation factor 2α (Eif2α). Phospho-Eif2α then acts to selectively inhibit translation, thereby controlling and reducing input into ER (41). Phospho-Eif2α also activates the downstream effector, Atf4, which induces targets including stanniocalcin 2 (Stc2) (involved in regulating Ca^{2+} homeostasis (62)), Atf3, c/ebp homologous protein (Chop), and growth arrest and DNA damage-inducible protein 34 (Gadd 34) (45). The latter of these are involved in promotion of proapoptotic pathways.

1.5.3.3 Atf6

Atf6 is an integral ER transmembrane glycoprotein that is constitutively expressed as a 90kDa protein (63). ER stress causes Atf6 to undergo cleavage by Site-1 and Site-2 proteases in the Golgi apparatus (64). The cytosolic N-terminal of Atf6 that contains a basic-leucine zipper motif is released as a 50kDa fragment and translocates to the nucleus, where it is acts as a transcription factor (63). Atf6 potentially induces the expression of UPR target genes including Xbp1-u, thereby acting in concert with activated Ire1α by providing the substrate for splicing (53).

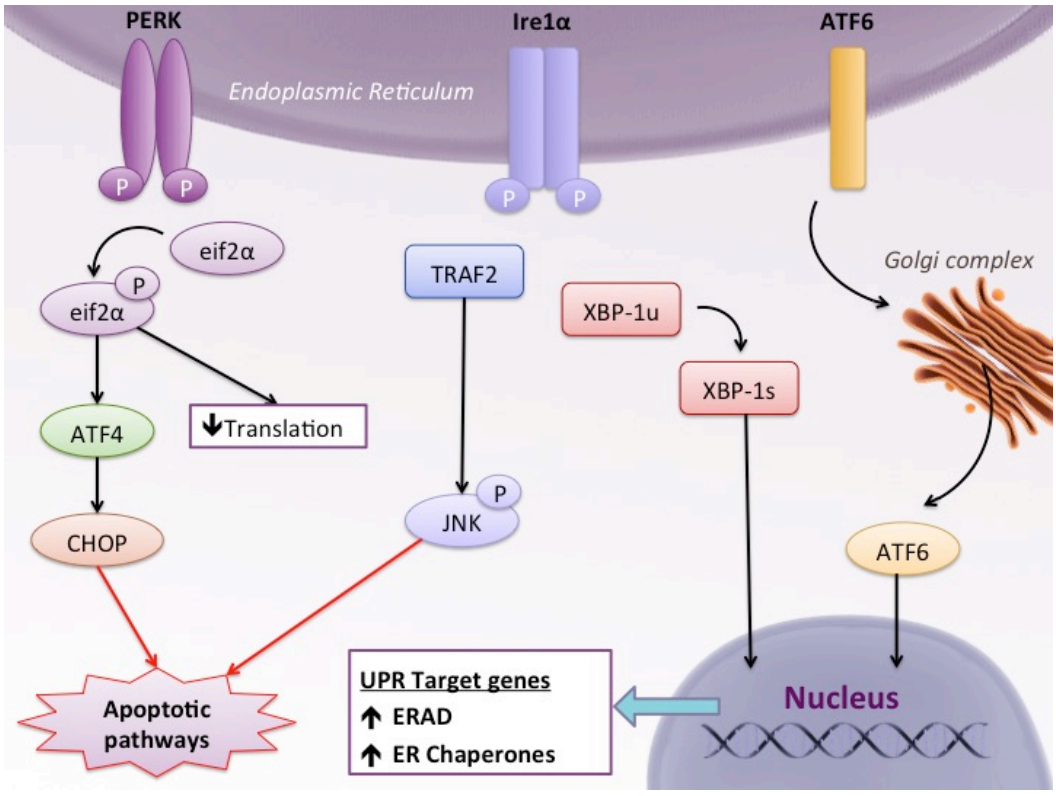

Figure 1.3 Simplified overview of UPR sensor pathways, adapted from (44)

1.5.3.4 Cell fate decisions

It has been well characterised that the Perk arm of the UPR can stimulate proapoptotic pathways under conditions of chronic ER stress (65). The Ire1α branch of the UPR is also able to interact with proapoptotic pathways through the association of Tnf receptor associated factor (Traf), leading to downstream phosphorylation of Jun-amino-terminal kinase (Jnk) (44, 66). Further identification small molecules that have the potential to preferentially induce distinct branches of the UPR may provide more insight into the contributions of each UPR pathway in response to ER stress (67).

1.5.4 ER stress in disease

ER stress is known to contribute to many pathological conditions, particularly conditions where either cellular protein production is increased or dysfunctional, including viral, neurodegenerative processes, α1-antitrypsin disorder, retinitis pigmentosa and amyloidoses (45, 67). ER stress has also been reported to contribute to micro-vascular complications of hyperglycaemia in diabetes mellitus independently of oxidative stress (68). The role of ER stress in liver disease and metabolic disorders has been a subject of much interest in recent years (reviewed in (44, 47, 69)). The ER is more abundant in secretory cells with high levels of protein production; hepatocytes are the primary site of synthesis of many proteins including plasma proteins, clotting factors, complement cascade and acute phase proteins; it is therefore possible that ER stress contributes to the development and pathogenesis of NASH. Interestingly, there is growing evidence that saturated fatty acids induce ER stress *in vitro*, providing a potential mechanism by which steatotic hepatocytes may be subject to ER stress.

1.5.5 ER stress in human NAFLD

The expression and regulation of the ER stress response in human NAFLD has been investigated (70). Protein expression was assessed in 27 liver samples, separated into four groups as described above: Normal (n=7), steatotic (n=7), NASH and fatty (n=8) and NASH not fatty (n=5). Western blotting

demonstrated significantly increased levels of XBP1-s in NASH groups compared to control and levels of STC2 were significantly increased in the NASH (not fatty group) (70). Although strong expression changes were observed for ATF4 and CHOP in tissue from some NAFLD patients, results did not reach significance due to large variation (70). The ratios of phosphorylated to total protein for either EIF2α or JNK were not significantly different between groups (70). XBP1 immunohistochemistry demonstrated increased nuclear staining in steatosis compared to control, which was more prominent in NASH groups (70). Using gene set enrichment on 45 samples (divided into groups of normal, steatosis and NASH), the study found that both the ER stress/UPR and lipogenesis pathways were down regulated, whereas apoptosis and autophagy were upregulated in NASH compared to control (70). Autophagy was also upregulated in steatosis compared to control, which may be an adaptive response to lipotoxicity (70).

Microarray gene expression of ER stress/UPR components demonstrated significant reduced levels of ATF4 and XBP1 mRNA in NASH compared to control and steatosis groups (70). ATF6 mRNA was found to be increased in steatosis compared to control, but not in NASH. Levels of IRE1, PERK and JNK mRNA were not significantly different between groups. Levels of STC2 were increased, and EIF2α and CHOP mRNA were decreased in NASH compared to steatosis but not significantly different from control (70). Although protein levels of some ER stress markers were significantly increased, gene set analysis of the ER stress/UPR pathway demonstrated a pattern of transcriptional down regulation in NASH (70). The authors also suggest a negative feedback mechanism to explain the finding (70), which requires further investigation. Particularly, XBP1 mRNA was significantly reduced in NASH, whereas protein levels and nuclear staining were significantly increased; as the authors propose, an increase in the proportion of XBP1-s mRNA was not assessed and could account for this finding (70).

Puri *et al* 2008 evaluated the expression of ER stress markers in human NAFLD and tested the hypothesis that the UPR would increase with disease progression

(71). The study utilised liver biopsy specimens from patients with metabolic syndrome alone (control group; n=17), metabolic syndrome with steatosis (n=21) and metabolic syndrome with NASH (n=21), excluding any patients with evidence of bridging fibrosis or cirrhosis. Metabolic syndrome was evaluated using Adult Treatment III criteria of abdominal obesity, hypertriglyceridaemia, lowered levels of high-density lipoprotein cholesterol, hypertension and impaired fasting glucose (72). NAFLD was diagnosed clinically as the elevation of enzymes or ultrasound evidence of fatty liver with exclusion of other aetiologies, including alcohol; these were assessed histologically and separated into steatosis and NASH groups. Histological parameters were qualitatively assessed and samples were scored quantitatively using the NAS. The study assessed expression of classical UPR pathway components: EIF2α, ATF4, XBP1, BIP, EDEM, CHOP and GADD34 (72). Apoptosis was investigated by assessing expression of classical pathway components, phospho-JNK and p38 mitogen-activated protein kinase (MAPK), alongside TUNEL (terminal deoxynucleotidyl Transferase dUTP Nick-End Labeling) assay. TUNEL assay is used to identify apoptotic cells through detection of nicks, damage and fragmentation of double-stranded DNA (73).

Results demonstrated that phospho-EIF2α was significantly increased in patients with NAFLD compared to metabolic syndrome alone (72). However, levels of downstream targets - ATF4 (mRNA and protein), CHOP and GADD34 (both mRNA) were not significantly different between groups or control (72). Levels of XBP1-u mRNA and protein were increased in patients with steatosis compared to control; there was also trend of increased XBP1-u mRNA in NASH compared to steatosis, however this did not reach statistical significance (72). XBP1-s mRNA was not different between groups, despite findings of individual NAFLD patients with highly increased levels, however this was found to directly correlate with histological severity (assessed by NAS) (72). Interestingly, XBP1-s protein expression was significantly reduced in NASH (72). A trend of increasing EDEM mRNA was also noted with disease progression. BIP mRNA was increased in NASH compared to the steatosis group, but was not significantly different from control. Levels of phospho-JNK were significantly

increased in NASH alone, p38 MAPK activity was increased in both steatosis and NASH groups compared to control and TUNEL assay also demonstrated an increasing apoptotic activity in steatosis and NASH (72).

These results demonstrate the complexity and variability of the human disease, but indicate the potential role of ER stress in human NAFLD.

1.5.6 ER stress and fatty acids

Wang *et al* 2006 investigated the effects of different dietary components used to induce hepatic steatosis in rats (74). The group compared the effects of three diets, rich in sucrose, saturated fatty acids (SFA; lard), and polyunsaturated fatty acids (PUFA; corn oil) respectively, against control diet in rats for up to 24 weeks. The study assessed lipid levels, responses to insulin challenge and mitochondrial integrity as well as hepatic expression of ER stress markers Bip, Chop and Xbp1-s. Rats were also challenged with partial hepatectomy and lipopolysaccharide (LPS) isolated from *Escherichia coli*.

Results demonstrated significantly increased hepatic triglycerides in all three dietary groups compared to control, with SFA and sucrose diets displaying higher levels than the PUFA group (74). Fat mass was significantly increased in the SFA and PUFA diets at 24 weeks. Despite basal similarity in glucose and insulin levels, the three experimental diet groups showed significantly reduced response to insulin during euglycaemic hyperinsulinaemic clamp studies (74). Mitochondrial integrity, assessed by JC-1 fluorescence (a dye that detects alterations in mitochondrial membrane potential), was reduced at 4 and 24 weeks by all diets compared to control; for both insulin response and mitochondrial integrity, no differences were noted between the three diets investigated (74).

Hepatic levels of Xbp1-s, Bip and Chop in were significantly increased by the sucrose and SFA diets (74). Caspase-3 activity was also increased in these two groups compared to control and PUFA diets, and these results were supported by isolated hepatocyte studies. After 1 week of respective diets, rats underwent partial hepatectomy. Following this, liver weight recovery was delayed in the three diet groups compared to control, and to a greater extent in the SFA group

and sucrose fed rats, supported by estimates of cell proliferation (74). Serum levels of AST and ALT were used to assess the response to LPS; enzymes were significantly more increased in SFA fed groups, and were also increased basally in these two diet groups (74). These results demonstrate that ER stress is increased in models of steatosis induced by both a sucrose rich diet and by diet rich in SFA (74). The same dietary groups that had increased ER stress markers also showed less capacity to respond to further insult in the form of partial hepatectomy.

The same group examined the effects of selected SFA and unsaturated fatty acids on ER homeostasis *in vitro* (75). Using a rat hepatoma cell line, Wei *et al* showed that ER stress was induced by incubation with the SFA palmitate or stearate, but not by the unsaturated fatty acids oleic acid or linoleic acid (75). The study utilised known pharmacological ER inducers thapsigargin and tunicamycin as positive control treatments.

Treatment for 6 hours with palmitate or stearate induced phosphorylation of Ire1α and Xbp1-splicing, and Eif2α phosphorylation was stimulated in a time dependent manner, in keeping with positive control cells. Saturated fatty acid treatment also increased mRNA of the ER stress markers Atf4, Chop, Bip and Gadd34; this differed from thapsigargin and tunicamycin treatments, which induced a larger range of ER stress markers. Cells incubated in either of the unsaturated fatty acids investigated, or thapsigargin, demonstrated increased caspase activity at 6hours; DNA laddering (a marker of apoptosis) and reduced cell viability was observed at 16hours. Co-treatment with the caspase inhibitor prevented these effects, but did not have any significant effect on the induction of ER stress markers.

Cellular concentrations of ceramide were increased with saturated fatty acid incubations, so a known inhibitor of ceramide synthetase (fumonisin B1) was used to test whether the observed induction of ER stress markers was a result of ceramide production. Although the inhibitor prevented increases in ceramide concentration, this did not have significant effect on ER stress markers or DNA

laddering. This indicates that ER stress induction and apoptosis occurred independently of ceramide.

No increase in markers of ER stress, apoptosis or cell viability were observed with either of the unsaturated fatty acids tested. In fact, addition and titration of oleic acid or linoleic acid was able to attenuate or prevent increases in mRNA and DNA laddering induced by palmitate. This study provides further evidence of a correlation between saturated fatty acids and induction of ER stress, and also demonstrates the potential importance of dietary saturated and unsaturated fatty acid composition in human NAFLD. From the data of mRNA induced by saturated fatty acids (particularly Atf4, Chop and Gadd34), it is possible that the unsaturated fatty acids palmitate and stearate may induce the PERK arm preferentially over other UPR pathways.

Palmitate has also been shown to induce lipid accumulation, ER stress, apoptosis and cell death in cardiomyocytes *in vitro* (76). In keeping with other studies, these effects were completely ameliorated by co-administration of oleate. ER stress markers were increased in a dose and time dependent manner by palmitate: Interestingly, Bip mRNA levels were significantly increased but Bip protein levels where only marginally elevated by palmitate. The authors tested the hypothesis that palmitate induced Bip degradation through proteasomal ubiquitination, by blotting for ubiquitin in Bip immuno-precipitates. The study demonstrated that the ubiquitin signal in isolates from palmitate treated cells was significantly increased compared to isolates from both positive (tunicamycin treated) and untreated control cells. This finding suggests that Bip may be under post-transcriptional regulation through the ubiquitin-proteasome pathway.

Interestingly, the study by Haffar *et al* demonstrated distinct staining patterns between cells treated with palmitate, compared to oleate and bovine serum albumin (BSA)-control cells (76). Although total levels of fatty acid uptake and total TG content were confirmed to be similar, oleate resulted in small, bright spherical pattern of lipid staining, described as consistent with droplet morphology, whereas palmitate staining was characteristically diffuse and faint,

with some spherical morphology but also demonstrate numerous non-spherical and irregular objects. Due to the nature of the staining, the authors suggest that palmitate may accumulate in the ER, potentially disrupting ER homeostasis through direct lipotoxicity. This requires further confirmation, but could explain the mechanism by which ER stress is caused by palmitate. Cardiovascular mortality and morbidity is increased in NAFLD and TIIDM, and TIIDM is also associated with steatotic cardiomyopathy. It is therefore possible that a common mechanism of ER stress induced by palmitate lipotoxicity may take place in the liver and cardiac tissue of patients with features of the metabolic syndrome.

Pharmacological induction of ER stress causes hepatic steatosis in rodent models (77, 78). Rutkowski *et al* investigated the relationship between ER stress and metabolism by assessing the effect of ER stress on mice deficient in distinct components of the UPR (78). Results showed that following tunicamycin challenge, Atf6α-null mice, $p58^{IPK}$-null mice, mice with liver specific Ire1α deletion and Eif2-mutant mice all developed hepatic steatosis. While wild type (WT) counterparts were able to resolve ER stress, these deficient mice all developed persistent UPR activation, demonstrated by upregulation and nuclear localisation of Chop at 48hours (78).

In response to tunicamycin, the livers of Atf6α-null mice showed microvesicular steatosis and an increased loss of structural ER integrity compared to WT mice. Atf6α-null mice also developed other features of metabolic disturbance, becoming hypoglycaemic and more severely insulin resistant than WT mice. Atf6-null mice also demonstrated increased reductions in serum levels of low and very low density lipoprotein (LDL and VLDL, respectively) following tunicamycin treatment, compared to WT mice (78).

Microarray profiling demonstrated similarity in basal gene expressions between WT and Atf6α-null mice (78). Tunicamycin challenge resulted in the transcriptional upregulation of numerous ER stress markers in WT mice, some of which were attenuated in Atf6-nulls (specifically Edem, Pdi family members PdiA4 and PdiA2, and co-chaperones $p58^{IPK}$ and Endoplasmin). However, in

both WT and Atf6-null mice, tunicamycin treatment resulted in the suppression of a number genes involved in metabolism and lipid homeostasis, including Srebp1, C/ebp, Pparα, Pparγc1, Foxo1, microsomal triglyceride transfer protein (Mttp), Fasn and fatty acid desaturase enzymes (78). Furthermore, while these changes were attenuated by 48hrs in WT mice, mice lacking UPR components demonstrated continued suppression of a number of metabolic transcriptional regulators including Srebp1, C/ebpa, Pparα, Pparγc1 and Chrebp (78). Expression of transcriptional target genes involved in fatty acid oxidation, lipogenesis, gluconeogenesis and lipoprotein synthesis pathways were also reduced (78). The authors suggest from the pathways inhibited that the accumulation of hepatic TG may result from reduced fatty acid oxidation rather than increased lipogenesis or uptake, although this warrants further investigation (78).

Similar patterns of gene suppression were found in $p58^{IPK}$-null, Ire1α-null and Eif2-mutant mice, leading the authors to conclude that metabolic dysfunction was due to ER stress rather than any specific pathway of the UPR (78). The study showed *in vitro* that levels of C/ebp were significantly reduced by actinomycin D (a translational inhibitor), indicative of a pattern of constitutive expression and basal degradation; therefore suppression under conditions of ER stress would result from inhibition of synthesis rather than increased degradation (78). The study assessed the response of Chop-null mice to tunicamycin and found that Chop-null mice had less hepatic lipid accumulation and suppression of metabolic regulators was attenuated. Therefore it is possible that Chop acts to suppress other C/ebp family members following ER stress (78) . The study concluded that suppression of metabolic genes is directly related to the hepatic ER stress response, and that metabolic dysfunction is perpetuated in conditions of unresolved ER stress (78).

Jo et al found that hepatic mRNA expression of ER stress markers (Bip, Chop, Dnajb9, Xbp1-s) were significantly induced alongside steatosis by tunicamycin in a mouse model (77). Expression of ER stress markers was not increased in adipose tissue. The study investigated the potential roles of lipogenesis, fatty

acid oxidation and lipid in a mouse model of pharmacological induced ER stress and steatosis. Results demonstrated suppression of the lipogenic genes Srebp-1c, Fasn and stearoyl-CoA desaturase 1 (Scd1) in the liver and expression of genes involved in fatty acid oxidation was not consistently different. Lipid delivery genes also showed a mixed pattern, however levels of hepatic VLDL receptor (VLDLR) mRNA were significantly increased. Expression of VLDLR was induced by tunicamycin in primary hepatocytes and MEFs, but not in two adipocyte cell lines (77).

In primary hepatocytes, actinomycin D (an antibiotic agent that acts as a transcriptional inhibitor) was able to repress both ER-stress induced triglyceride accumulation and expression of VLDLR, Bip and Dnajb9 (77). Treatment with cycloheximide, a protein synthesis inhibitor, was also able to repress pharmacological ER stress mediated TG accumulation *in vitro*. The authors suggest these results demonstrate 1) that transcriptional upregulation of VLDLR, and 2) newly synthesised proteins, respectively, are required for tunicamycin induced triglyceride accumulation (77). However, the strong possibility that both actinomycin and cycloheximide are acting to alleviate ER stress, via reduction of transcriptional demand and input into the ER or by alternative pathways must also be considered.

Interestingly, suppression of VLDLR via small interfering RNA (siRNA) or in primary hepatocytes from VLDLR-deficient mice was able to alleviate intracellular triglyceride accumulation, supporting the potential role of VLDLR in steatosis (77). The study demonstrated that suppression of the Perk pathway (rather than Ire1α or Atf6 arms of the UPR) attenuated VLDLR expression induced by ER stress in murine epithelial fibroblasts and primary hepatocytes (77). Furthermore, overexpression of Atf4 increased VLDLR expression. This suggests possible cross-talk between the Perk arm of the UPR and lipid delivery pathways, supported by the presence of two conserved Atf4 binding motifs in the promoter region of the murine VLDLR gene (77).

The effects of tunicamycin treatment were assessed in VLDLR-deficient mice; although mRNA expression of ER stress markers was comparable to WT, hepatic triglyceride in VLDLR-deficient mice increased to a significantly lesser extent (77). Similarly, when fed a high fat diet VLDLR-deficient mice accumulated less hepatic triglyceride than wild type counterparts. Results from an *in vivo* detergent assay showed suppression of VLDL secretion by tunicamycin in both WT and VLDLR-deficient mice (77). Taken together, these results suggest that VLDLR contributes to the development of hepatic steatosis induced by pharmacological ER stress and high fat diet. The results are suggestive of an increased role of lipid delivery, rather than reduced secretion, metabolism or increased lipogenesis (77).

These laboratory studies support the hypothesis that ER stress has a role in the pathogenesis and progression of NAFLD, by providing evidence of associations between ER stress, metabolic alterations and TG accumulation. The results also demonstrate how dietary factors relating to SFA and PUFA could potentially be responsible for some of the heterogeneity in the NAFLD patient population.

1.6 AIMS OF RESEARCH

Several complex and interacting signaling networks may be relevant in the development of NAFLD; discerning the ways in which each of these mechanisms may cause dysfunction and contribute to pathogenesis may be key to prevention, treatment and reducing the significant burden of this increasingly common disease. This project primarily focuses on oxidative stress and ER stress –these may have a role in the pathogenesis of NASH and cross talk between components of these complex signaling pathways is likely. Although it is known that Nrf2 has a key role in cellular defence against oxidative stress, the role of Nrf2 in different environments of cellular stress has not been fully explored. Liver and adipose tissues from a dietary mouse model of NASH have been used to assess the role of Nrf2 in inflammation, ER stress and metabolic disturbance. A cell culture model has been used to further elucidate mechanisms of cellular crosstalk between ER and oxidative stress pathways.

Therefore, this project has two aims:

1. To further explore the role of Nrf2 in NAFLD by examining the effect of pharmacologically upregulated Nrf2 on metabolic, inflammatory and ER stress markers in a dietary induced mouse model of NASH.
2. To investigate the role of Nrf2 in response to ER stress *in vitro*.

Chapter 2 Methods and materials

2.1 Materials and Reagents

Materials used were from SigmaAldritch unless stated otherwise. The recipes of buffers and solutions commonly used in this project are described in Table 2.1.

Table 2-1. Details of buffers and solutions used in this project

Buffer	Constituent materials
RIPA buffer	50mM Tris, 150mM NaCl, 0.1%SDS, 0.5% sodium deoxycholate, 1% Triton X 100
Modified RIPA buffer	10ml RIPA, 50ul 200mM sodium orthovanadate, 10ul 1M dithiothreitol, 1 tablet complete mini EDTA-free cocktail protease inhibitor (Roche Diagnostics), 100ul Halt TM single use cocktail phosphatase inhibitor (ThermoScientific).
10X Transfer buffer (TB)	Tris 300g, Glycine 1440g, fill to 10L with dH_2O
SDS Running buffer	10% (v/v) 10% TB, 1% (w/v) SDS in dH_20
MOPS running buffer	1% (v/v) 3-(N-morpholino)propanesulfonic acid in dH_20
Transfer buffer	20% (v/v) methanol, 10% 10X TB, 0.1% SDS in dH_20
RLT buffer	10ml RNEasy Mini Kit RLT (Qiagen), 10ul mercaptoethanol
Enhanced chemiluminescence (ECL) solution 1	500ul 250mM luminol in DMSO, 220ul 90mM coumaric acid in DMSO, 5mL 1M Tris HCl pH8.5 made up to 45ml with dH_20 (Stored in the dark at 5C)
Sodium dodecyl sulfate (SDS) polyacrylamide gels	Polyacrylamide Ultra Pure ProtoGel (National Diagnostics), 1.5M Tris-HCl pH8 or 1.0M Tris-HCl pH6.5, 10% (w/v) SDS, N,N,N',N'-Tetramethyl-ethylenediamine (Sigma), 1% ammonium persulphate

(Proportions according to standard protocols)	in dH_2O
Tris buffered saline tween (TBST)	20X TBS: Tris-HCl 48.4g, NaCl 192g, pH7.6 TBST: 1X TBS, 0.1% (v/v) tween-20.
BSA blocking buffer	5% w/v BSA in TBST
ECL solution 2	32uL 30% hydrogen peroxide, 5ml 1M Tris HCl pH8.5 made up to 45ml with dH_2O. (Stored in the dark at 5C)

2.2 Animal experiments

Prior to starting in the lab, wild type C57Bl6 mice were separated into two age- and weight-matched groups and placed onto either 1) normal chow (NC) or 2) a high fat diet with high fructose in drinking water (HFFr), for 24 weeks. The HFFr mice were fed a diet comprised of 60% fat and were given drinking water containing 30% fructose. Within in each group, mice were treated for a further six weeks with either the compound TBE-31, a pharmacological Nrf2 up-regulator, or with dimethyl sulfoxide (DMSO) for control. TBE-31 was given to mice via oral garage 3 times a week at a concentration of 5nmol/g body weight.

There were 4 groups based on diet (NC or HFFr) and treatment with (+) or without (-) TBE-31. At 30 weeks, the mice were culled using a schedule 1 protocol, and tissues were collected. Animals were treated and housed humanely and in accordance with the UK Animals (Scientific Procedures) Act, 1986. Liver and adipose tissue samples were kindly received from Dr Ritu Sharma (Hayes Lab). Other results from the Hayes Lab indicated that the effect of the HHFr diet on wild type mice closely resembled the human NASH phenotype, with hepatic steatosis, inflammation and insulin resistance.

2.3 Cell culture

Immortalised mouse epithelial fibroblasts (MEF) cells were maintained in Iscove's Modified Dulbecco's Medium (IMDM), supplemented with 10% fetal calf serum (FCS), 1% 100X Insulin-transferrin-selenium (ITS) (final concentrations of 0.01mg/ml insulin, 5.5ug/ml transferrin and 6.7ng/ml sodium

selenite) and 1.5nM recombinant human epidermal growth factor (EGF) (all from ThermoFisher Scientific). Culture flasks and wells were coated with 0.1% gelatine in phosphate buffered solution (PBS) for at least 30mins at room temperature; this was removed prior to seeding. Immortalised wild type (WT), $Nrf2^{-/-}$ cells and $Keap1^{-/-}$ cells were kindly received from the Dinkova-Kostova Lab. These were cultured and maintained at 37°C with 5%CO_2.

2.3.1 Treatment conditions: ER stress induction

2.3.1.1 Initial glucose starvation and tunicamycin studies with WT and $Nrf2^{-/-}$ MEFs

MEF cells were seeded into 6 well plates the following seeding densities and labelled accordingly: WT $3x10^5$/well and $Nrf2^{-/-}$ $5x10^5$/well. Cells were left overnight, before being treated with 0.5ml/mg of sulforaphane (kindly received from the Dinkova-Kostova lab) or dimethyl sulfoxide (DMSO) for control, in fresh supplemented IMDM media (as above). After 3 hours of treatment, media was removed, cells were washed twice with phosphate buffered saline (PBS) and time 0 (T=0) was recorded.

2.3.1.2 Experiment 1. Glucose deprivation time-course

At T=0, cells were incubated in glucose free Dulbecco's Modified Eagle Medium (DMEM) (ThermoFisher Scientific), without FCS, supplemented with either 0.5ml/mg sulforaphane or DMSO. Cells were collected in RIPA buffer at specific time points; T=0, 1, 2, 4, 6, 8 hours. At each time point, 2 wells of cells were collected (with the exception of the $Nrf2^{-/-}$ 8 hour time point).

2.3.1.3 Experiment 2. Tunicamycin treatment

At T=0, cells were incubated in supplemented IMDM as described above, with the addition of either 1) Tunicamycin (Sigma) at concentration of 5ug/ml or DMSO for control. Sulforaphane or DMSO control treatments were also added to the fresh media and continued throughout the experiment. After 6 hours, 2 wells of cells were collected for each treatment group.

After preliminary experiments, it was decided to utilise a longer pre-treatment of 16-24hours with sulforaphane 0.5ul/ml or DMSO vehicle control and to

discontinue this during ER stress induction. This was to eliminate any potential interactions between Tunicamycin and Sulforophane during ER stress induction and provide more useful information. The cells seeding densities were also amended to reflect the longer treatment to: WT $2x10^5$/well and Nrf2$^{-/-}$ $3.5x10^5$/well.

2.3.1.4 Experiment 3. Glucose starvation time-course

Cell seeding was followed as above, with the addition of Keap1$^{-/-}$ MEF cells at density of $1.5x10^5$/well. Cells were left overnight before being treated with 0.5ul/ml of sulforaphane or DMSO control in fresh media. After 16 hours of treatment, cells were washed twice with PBS before incubation in glucose free DMEM only. Cells were collected at the specified time-points, with 2 wells pooled for each time point for protein analysis.

2.3.1.5 Experiment 4. Tunicamycin treatment

Cell seeding and sulforaphane pre-treatment was followed as previously described. After 16 hours of treatment, cells were washed twice with PBS and then incubated in supplemented IMDM media with Tunicamycin 5ug/ml or DMSO. After 6 hours, 3 wells were pooled for each treatment for protein analysis. This experiment was performed in duplicate.

2.3.1.6 Experiment 5. Treatments for mRNA collection

WT and Nrf2$^{-/-}$ MEF cells were seeded into 6 well plates as above. After settling overnight cells were washed twice with PBS. Cells were then treated with either: 1) supplemented IMDM media; or 2) glucose free DMEM supplemented with 10% FCS only; or 3) supplemented IMDM media with 5ug/ml Tunicamycin. Cell lysates were collected at specified time-points using 100ul of RT buffer (Qiagen) plus EDTA (0, 6, 12 and 24 hours), and 2 wells of cells were pooled for mRNA analysis.

2.4 Protein lysate preparation and immunoblotting

2.4.1.1 Adipose tissue preparation

Protein lysates were prepared from adipose tissue samples from 3 mice in each group: Tissue was homogenised in 600uL of modified RIPA buffer (as described

above, plus 20ul 0.1M phenylmethylsulfonyl fluoride). Samples were then centrifuged at 4°C for 15mins and the cytoplasmic extract was isolated.

2.4.1.2 MEF cell lysates

Cells were collected using modified radioimmunoprecipitation assay (RIPA) buffer, as described in Recipes. Samples were placed on ice before undergoing protein estimation or were frozen in liquid nitrogen and stored at -20°C.

2.4.3 Quantitative protein estimation

Protein estimation was performed using the detergent-compatible (DC) assay; absorbances were performed in duplicate and used to calculate sample protein content by comparison to bovine serum albumin (BSA) standards of known concentration. Protein levels of lysates were normalised and prepared for immunoassay with the addition of 4X lithium dodecyl sulphate sample loading buffer, 20X sample reducing agent (both NuPAGE, Invitrogen) and dH_20.

2.4.4 Western blotting

Electrophoresis was used to separate proteins in the protein lysate in sodium dodecyl sulfate (SDS)-polyacrylamide gels, or pre-cast Bis-Tris 4-12% Midi gels (Novex). SDS-PAGE casting followed standard Laemmli protocols; buffers used are described in recipes section and gel percentages and electrophoresis conditions were optimised for sample numbers and the proteins of interest. Standard running conditions were 200V for 55mins, and gels were transferred to polyvinylidene difluoride membranes at 60V for 75mins. Membranes were blocked in 5% BSA or 5% powdered milk in tris-buffered saline with tween (TBST) for at least 1 hour before placement into primary antibody. Membranes underwent thorough washing in TBST between placement in primary and secondary antibodies, and prior to enhanced chemiluminescence (ECL) development. Blots were developed by exposure to film in a darkroom following ECL application, for certain primary antibodies blots were developed with sensitive Immobilon Chemiluminescent HRP substrate (Millipore). Results were assessed with densitometry using Image J software and normalised relative to sample β-actin levels.

2.4.5 Antibodies

Primary antibodies detailed in Table 2.2 below were used to detect a panel of proteins involved in ER stress, inflammation and fatty acid metabolism. Monoclonal antibody against β-actin was used to assess protein-loading levels.

Table 2-2. Details of primary antibodies used in this project

Primary antibody	Size (kDa)	Company	Species	Type
Nqo1	31	In-house	Rabbit	Monoclonal
Actin-beta (HRP)	39	Sigma	Mouse	Monoclonal
Xbp1	29 40	Abcam	Rabbit	Polyclonal
Il6	23	Abcam	Rabbit	Polyclonal
Jnk	46 54	Cell Signaling Technology	Rabbit	Polyclonal
phospho-SAPK/Jnk (Thr183/Tyr185)	46 54	Cell Signaling Technology	Rabbit	Polyclonal
Tnfα	17 25	Cell Signaling Technology	Rabbit	Polyclonal
Acaa1	44	ThermoScientific	Rabbit	Polyclonal
Scd-1	37	Cell Signaling Technology	Rabbit	Polyclonal
Acox1	74	Abcam	Rabbit	Polyclonal
Fabp	10-15	Abcam	Rabbit	Polyclonal
Ces1	~60	ThermoScientific	Rabbit	Polyclonal
Pparα	52	Abcam	Rabbit	Polyclonal
Chop	27	Cell Signaling Technology	Rabbit	Monoclonal
Eif2α	38	Cell Signaling Technology	Rabbit	Polyclonal
phospho-Eif2α (ser51)	38	Cell Signaling Technology	Rabbit	Polyclonal
Pdi	57	Cell Signaling Technology	Rabbit	Monoclonal
Ero1-Lα	60	Cell Signaling Technology	Rabbit	Polyclonal
Bip	78	Cell Signaling Technology	Rabbit	Polyclonal
Perk	140	Cell Signaling Technology	Rabbit	Monoclonal
phospho-Perk (Thr980)	170	Cell Signaling Technology	Rabbit	Monoclonal
Ire1α	130	Cell Signaling Technology	Rabbit	Monoclonal
Xbp1-spliced	54	BioLegend	Rabbit	Polyclonal

Atf4	49	Cell Signaling Technology	Rabbit	Monoclonal
Atf6α	50 (f) 90	Santa Cruz Biotechnology	Rabbit	Polyclonal
phospho-Ire1α (Ser724)	110	ThermoScientific	Rabbit	Polyclonal
$P58^{IPK}$	58	Cell Signaling Technology	Rabbit	Monoclonal
Nrf2	97-100	Cell Signaling Technology	Rabbit	Monoclonal

2.5 Quantitative reverse transcription polymerase chain reaction (qRT-PCR)

The RNeasy Mini Kit (Qiagen 74104, 74107) was used to prepare cDNA from sample mRNA following manufacturer's protocols. A nanodrop spectrophotometer was used to estimate RNA in samples. cDNA was prepared from mRNA using the Omniscript RT 200 kit (Qiagen) as per instruction, it was assumed that 1ug RNA would produce 1ug cDNA. For animal tissue experiments, mRNA previously extracted from mouse liver tissue was used to prepare cDNA. The number of samples from each treatment group was as follows: NC(-) 7, NC(+) 8, HFFr(-) 7, HFFr(+)7.

Standard qRT-PCR was performed using 12.5uL of probe mix (comprised of 4.5ul Taqman Universal Master Mix II, no UNG (Applied Biosystems), 0.75ul of specific probe and made up to 12.5uL with dH_20), with 2.5ug of sample cDNA. (Amounts of dH2O and cDNA were adjusted for some probes.) Probes used are listed in Table 2.3. SYBR Green PCR Master Mix (Applied Biosystems) was used for reverse and forward Xbp1-s primers. Triplicates were performed for each sample, and actin and/or S18 were used as housekeeping genes. Plates were sealed and centrifuged at 1980g for 3mins. Samples were then run using 7500 Real-Time PCR System (Applied Biosystems) on a standard 90min qRT-PCR cycle.

Table 2-3. Details of probe primers used for rt-qPCR

Probe primer	**Assay ID** (Applied Biosystems)	**Label**
18S	4319413E	VIC
F4/80	Mm00802529_m1	Fam
B220	Mm01293577_m1	Fam
Nos2	Mm00440502_m1	Fam
Gsr	Mm00439154_m1	Fam
Pparγc1	Mm01208835_m1	Fam
G6pc	Mm00839363_m1	Fam

Cd68	Mm03047340_m1	Fam
Elovl6	Mm00851223_s1	Fam
Itgam	Mm00434455_m1	Fam
Cd36	Mm00432403_m1	Fam
Pparγ	Mm00440940_m1	Fam
Ccl2	Mm00441242_m1	Fam
Mpo	Mm01298424_m1	Fam
Rela	Mm00501346_m1	Fam
Perk	Mm00438700_m1	Fam
Ire1α	Mm00470233_m1	Fam
Atf4	Mm00515325_g1	Fam
Chop	Mm01135937_g1	Fam
Bip	Mm00517691_m1	Fam
$P58^{IPK}$	Mm01225042_m1	Fam
Erdj4	Mm01622956_s1	Fam
Dnajb11	Mm00518196_m1	Fam
Edem1	Mm00551797_m1	Fam
Serp1	Mm00472715_m1	Fam
Ero1α	Mm00469296_m1	Fam
Atf6	Mm01295319_m1	Fam
Atf3	Mm00476032_m1	Fam
Eif2α	Mm01289723_m1	Fam
Xbp1(total)	Mm00457360_m1	Fam
β Actin	Mm00607939_s1	VIC
Xbp-1 spliced	Xbp1 5' and 3' (SYBR) spliced – CTGAGTCCGAATCAGGTGCAG GTCCATGGGAAGATGTTCTGG	SYBR Green

2.6 Statistical analysis

All results are given in terms of relative fold change compared to WT control. Two-way ANOVA with Bonferroni post-test analysis was performed for rtPCR

data. Graphs and images were produced using ImageJ and Prism GraphPad software.

Chapter 3 Investigating the pathogenesis of NASH in mice fed a High Fat plus High Fructose diet

3.1 Introduction

The aim of this chapter is to investigate the role of Nrf2 using a diet induced mouse model of NASH. Experiments were performed to investigate the role of Nrf2 in NASH by assessing the effects of pharmacological up-regulation of Nrf2 by the compound TBE-31 in wild type mice with diet-induced NASH. TBE-31 is a potent Nrf2 activator through interaction with Keap1 (79). Mice were divided into 4 groups based on diet (NC or HFFr) and TBE-31 treatment:

1. NC (-) Normal chow diet with DMSO
2. NC (+) Normal chow diet with TBE-31
3. HFFr (-) High fat, high fructose diet with DMSO
4. HFFr (+) High fat, high fructose diet with TBE-31

RtPCR was performed on liver samples (NC(-) n=7, NC(+) n=8, HFFr(-) n=7, HFFr(+) n=7), to analyse hepatic mRNA expression of a selection of genes involved with inflammation, oxidative stress and metabolism. Western blotting was performed on adipose tissue (n=3 mice per intervention group) to assess protein expression of ER stress markers, inflammatory proteins and metabolic pathways.

3.2 Results

3.2.1 Comparison of mRNA expression in the liver

The graphs presented in Figure 3.1 depict results for genes with reasonable interpretable data[2]. These results demonstrate that the mRNA levels of nitric oxide synthase (Nos2), macrophage marker F4/80 and B-lymphocyte marker B220, are all upregulated in the livers of HFFr (-) mice, compared to control mice, suggestive of an inflammatory process within the livers induced by the HFFr diet. These increases were not found in the livers of HFFr (+) mice,

[2] Other genes assessed included: G6pc, Txn1, Gstm1, Mcr1, Atf3, G6pc, Cd68, Itgam, Cd36, Pparγ, Ccl2, Mpo and Rela.

implying that the addition of TBE-31 compound acted to attenuate an inflammatory process. As the TBE-31 compound activates Nrf2, it is possible that increased Nrf2 activity ameliorated the inflammatory changes induced by the HFFr diet. There is also a trend towards down-regulation in mRNA levels of Gsr, involved in glutathione recycling and Pparγc1, involved in defence against oxidative stress, in both HFFr (+) and HFFr (-) mice compared to NC mice. This could suggest either that mice fed the HFFr diet experience less oxidative stress, or that mice fed the HFFr diet have a reduced ability to respond to oxidative stress. Although the latter option is more in keeping with the increased markers of inflammation observed.

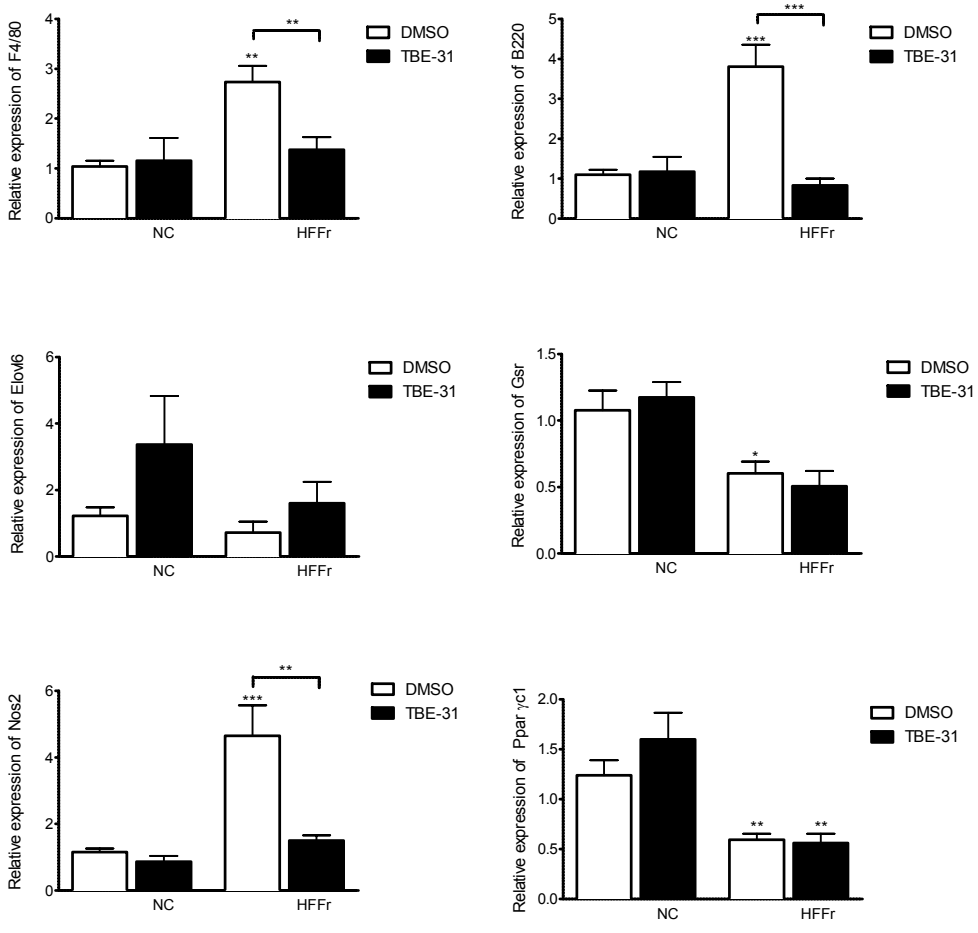

Figure 3.1. Relative expression of mRNA in the liver of mice on normal chow (NC) or high fat high fructose (HFFr) diets, with the addition of either DMSO (control) or the compound TBE-31.
N= 6-7 mice per group, significance compared to NC (DMSO) except where indicated with bars, *P ≤0.05; ** P ≤0.01; *** P ≤0.001

3.2.2 Comparative protein abundance in adipose tissue

Proteins assessed in adipose tissue included the inflammatory markers Jnk, phospho-Jnk and Il6. Many classical ER stress response proteins were analysed including components of the Perk arm of the UPR (Perk, phospho-Perk, Eif2α and Chop) as well as Xbp1 (Ire1α UPR pathway) and Atf6. Expression levels of ER redox enzymes Pdi and Ero1α were also investigated. Proteins involved in lipid homeostasis analysed included the lipogenic enzyme Scd1, involved in fatty acid biosynthesis. Lipid catabolism was investigated by assessing levels of the first and last enzymes in mitochondrial β-oxidation, acyl-CoA oxidase 1 (Acox-1) and acetyl-CoA acyltransferase (Acaa) respectively. Expression of Fabp was analysed, as was carboxylesterase 1 (Ces1), an enzyme involved in fatty acid mobilisation and VLDL secretion; Ces1 hydrolyses TG and is localised to the ER (80).

Individual variation between mice meant that none of the results from western blotting reached levels of statistical significance. The data from adipose tissue was found to be too variable to interpret and is therefore not shown.

3.3 Discussion

Experiments were performed to investigate the role of Nrf2 in NASH by assessing the effects of pharmacological up-regulation of Nrf2 in wild type mice by the compound TBE-31, with NASH induced by HFFr diet that closely resembled the human disease.

The results are suggestive of an inflammatory process occurring in the livers of mice on an HFFr diet, but this was not demonstrated in adipose tissue. It is possible that this may be related to the time course of the experiment: Stanton *et al* used a high fat and cholesterol diet to study NASH in mice, and demonstrated that inflammatory markers were up-regulated in adipose tissue and liver differentially, with adipose tissue typically showing inflammation earlier at 6-16 weeks, and the liver at later stages (26 weeks) (81). As the mice in the current study were culled after 30 weeks of NC or HFFr diet, this would reflect a later stage of disease. The lack of significant adipose tissue inflammation may also be due to the sample size of n=3 used in the current project.

ER stress and the adaptive pathways resulting in the UPR are known to affect lipid metabolism and steatosis (77). In experiments using an ER stress-inducing drug in mice, Jo *et al* (77) found that expression of ER response genes is not significantly altered in tissues other than liver, however this was using an ER stress inducer injected intra-peritoneally, which may have influenced more local effects on the liver. The lack of significant results of ER stress proteins in adipose tissue in this project may support this observation, as no clear evidence of UPR induction was demonstrated. However, analysis of a larger sample may reveal trends. The enzymes involved in metabolism and inflammation also did not show a clear pattern of expression in adipose tissue. However, this again may be related to the sample size used or the age of the mice in this study, and requires further investigation. These results demonstrate both the complexity of the interacting pathways involved in NASH, confounded by variation between individual mice.

Chapter 4 Unravelling the role of Nrf2 during endoplasmic reticulum stress *in vitro*

4.1 Introduction

The purpose of this study was to determine whether Nrf2 activity interacts with components of the UPR under conditions of ER stress, and to characterize the influence of Nrf2 during the cellular response to ER stress. ER stress markers and classical components of the UPR under conditions of ER stress were examined in cells that lacked Nrf2, or had pharmacologically or genetically upregulated Nrf2 activity.

This study utilized an *in vitro* model of mouse epithelial fibroblasts (MEFs), comparing control cells (WT) with cells lacking Nrf2 (Nrf2-knockout, $Nrf2^{-/-}$) and cells with increased Nrf2 activity due to loss of Keap1 suppression (Keap1-knockout, $Keap1^{-/-}$). The effect of pharmacologic Nrf2 up-regulation in ER stress was also assessed using WT cells pre-treated with the Nrf2 inducer (SFN). SFN is an isothiocyanate that activates Nrf2 through Keap1 (82). ER stress was induced using methods of glucose starvation and tunicamycin treatment (Tm): Glucose starvation produces ER stress via blocking N-linked glycosylation and reducing cellular ATP, tunicamycin treatment causes inhibition of first enzyme of glycoprotein synthesis, resulting in accumulation of glycoproteins within the ER (83). To detect ER stress and characterize the UPR, the mRNA and protein expression of a panel of well-established components of the unfolded protein response was analyzed using western blotting and quantitative real-time polymerase chain reactions (q-rtPCR).

4.2 Results

4.2.1 Confirming established Nrf2 cell status

Western blot and rtPCR data of the classical Nrf2 target, Nqo1 was assessed to confirm cells were expressing the expected Nrf2 phenotype. Results demonstrate that basal levels of Nqo1 were dependent on Nrf2 status, with both protein and mRNA extremely reduced in $Nrf2^{-/-}$ cells and strongly upregulated in $Keap1^{-/-}$

cells compared to WT. Nqo1 protein expression was also found to be up-regulated in SFN treated cells, indicating that the pretreatment was able to adequately activate Nrf2. Western blotting of Nrf2 also demonstrated increased levels in both Keap1$^{-/-}$ and SFN treated cells, and no expression in Nrf2$^{-/-}$, further confirming Nrf2 status in cells. Tunicamycin treatment had no evident effects on Nqo1 protein expression. These results can be observed in Figures 4.2-4.5 and 4.8.

4.2.2 The response of wild type MEF cells to ER stress

Western blotting results shown in Figures 4.1-4.4 demonstrated that components of the UPR were not highly expressed in WT cells at baseline. When WT cells were subject to ER stress, either by glucose starvation or tunicamycin treatment, there was prominent induction of Atf4, Bip and Chop, as well as increases in levels of Eif2α, Pdi, Perk and Ire1α.

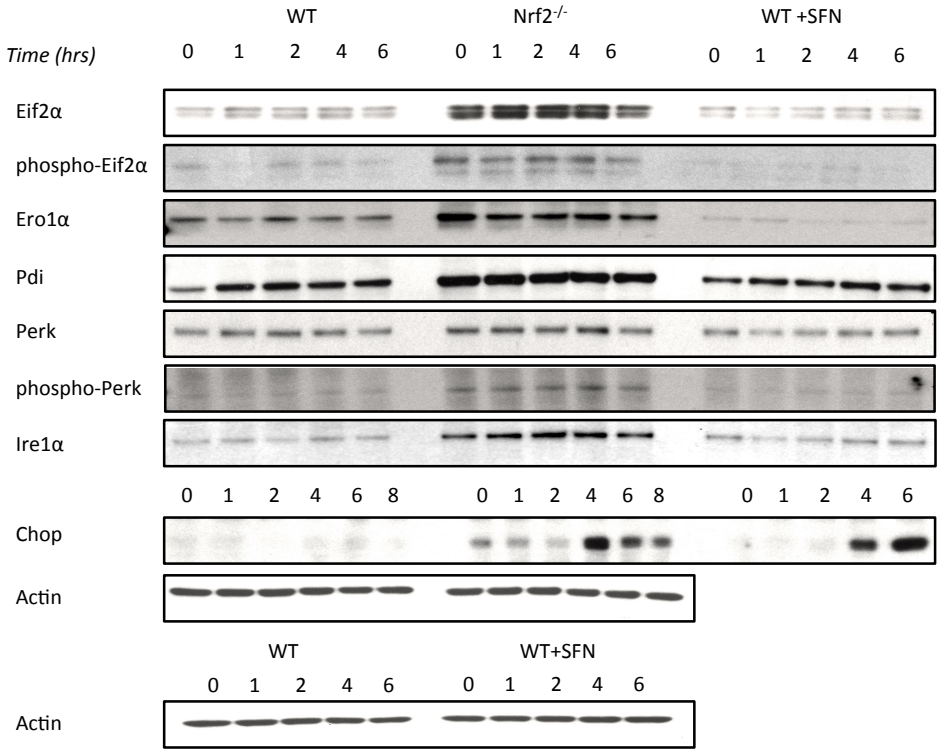

Figure 4.1 Western blot results of Experiment 1: Glucose starvation time course. ER stress response markers in MEF cells incubated in glucose-free DMEM for up to 6 hours. Key: WT= wild type; SFN = Sulforaphane

4.2.3 Components of the UPR are consistently upregulated in cells lacking Nrf2 under basal conditions

In Experiment 1 it was observed that cells lacking Nrf2 had upregulated protein expression of ER stress markers at baseline: Levels of Perk, Eif2α, phospho-Eif2α, Chop, Ero1α, Pdi and Ire1α were all increased at T=0 in $Nrf2^{-/-}$ cells, compared to WT. In keeping with these results, baseline protein levels of Pdi, Ire1α, Eif2α and phsopho-Eif2α were demonstrably increased in $Nrf2^{-/-}$ cells in Experiment 2. Chop was also increased basally, although this is not seen in Figure 4.2 due to differences in exposure. In addition, levels of both unspliced and spliced Xbp1 protein were basally increased in $Nrf2^{-/-}$ cells, providing further evidence that UPR components are basally upregulated in cells lacking Nrf2. The results of further glucose deprivation (Experiment 3, shown in Figure 4.3) and tunicamycin treatment (Experiment 4, shown in Figure 4.4) confirmed the finding that components of the UPR were raised at baseline in cells lacking Nrf2. Specifically, basal levels of Eif2α, phospho-Eif2α, Ero1α, Pdi, Ire1α and Xbp1-s were found to be consistently increased in $Nrf2^{-/-}$ cells. However, levels of Perk and phospho-Perk did not appear to be basally increased in $Nrf2^{-/-}$ cells in further experiments.

There are a number of possible reasons that could account for these findings. Components of the UPR may be constitutively activated in $Nrf2^{-/-}$ cells, or cells lacking Nrf2 may have heightened sensitivity to ER perturbations. Increased basal levels of Ero1α and Pdi could be caused by homeostatic readjustment to alterations in the ER REDOX homeostasis caused by reduced cellular antioxidant capacity (such as reduced glutathione), in the absence of Nrf2.

The upregulated protein levels of Perk, Eif2α, phospho-Eif2α and Chop suggests that lack of Nrf2 increases expression and/or activation of components of the Perk arm of the UPR. However, the general upregulation of other UPR components including Ire1α in $Nrf2^{-/-}$ cells suggest general induction of the UPR as well as Perk arm activation. It should also be noted that if $Nrf2^{-/-}$ cells are under constitutive ER stress, the Perk arm may be preferentially activated to stimulate pro-apoptotic pathways (65).

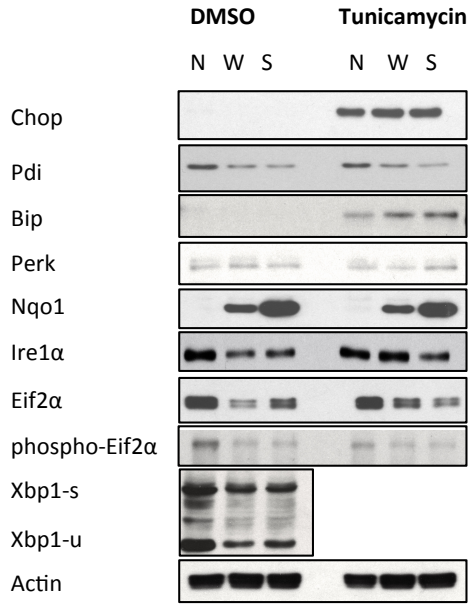

Figure 4.2. Western blot results of Experiment 2: ER stress response markers in MEF cells treated with Tunicamycin. Cells were treated with Tunicamycin or control (DMSO) for 6 hours. Key: N =Nrf2$^{-/-}$; W= wild type; S = WT + Sulforaphane.

4.2.4 The basal expression of ER stress markers in sulforophane treated WT cells

Experiment 1 demonstrated that WT cells treated with SFN had basally reduced protein expression of Eif2α, phospho-Eif2α and Ero1α compared to WT cells. Reduction of these ER stress markers in SFN treated cells indicates that pharmacologically upregulated Nrf2 reduces the basal expression requirement for ER homeostasis. Perk expression appeared to be similar to WT levels in SFN treated cells, which is surprising with the observed reduction in downstream effectors of the Perk UPR arm. In Experiment 2, basal protein expression of ER stress markers did not dramatically differ between SFN treated and WT cells, with the exception of Eif2α. In contrast to findings in Experiment 1, Eif2α protein level was initially increased in SFN treated cells compared to WT. These results are ambiguous, but raise the possibility that either increased Nrf2 activity (mediated by SFN) or SFN itself is moderating the Perk signalling cascade.

From initial results, it was postulated that the lack of Nrf2 might increase susceptibility to ER stress, and conversely that up-regulation of Nrf2 might

augment resistance to ER stress. Keap1$^{-/-}$ cells were introduced in Experiments 3 and 4 to test this hypothesis. A clear pattern with any specific arm of the UPR was not able to be confirmed, so a larger panel of ER stress markers and UPR components was assessed in further experiments.

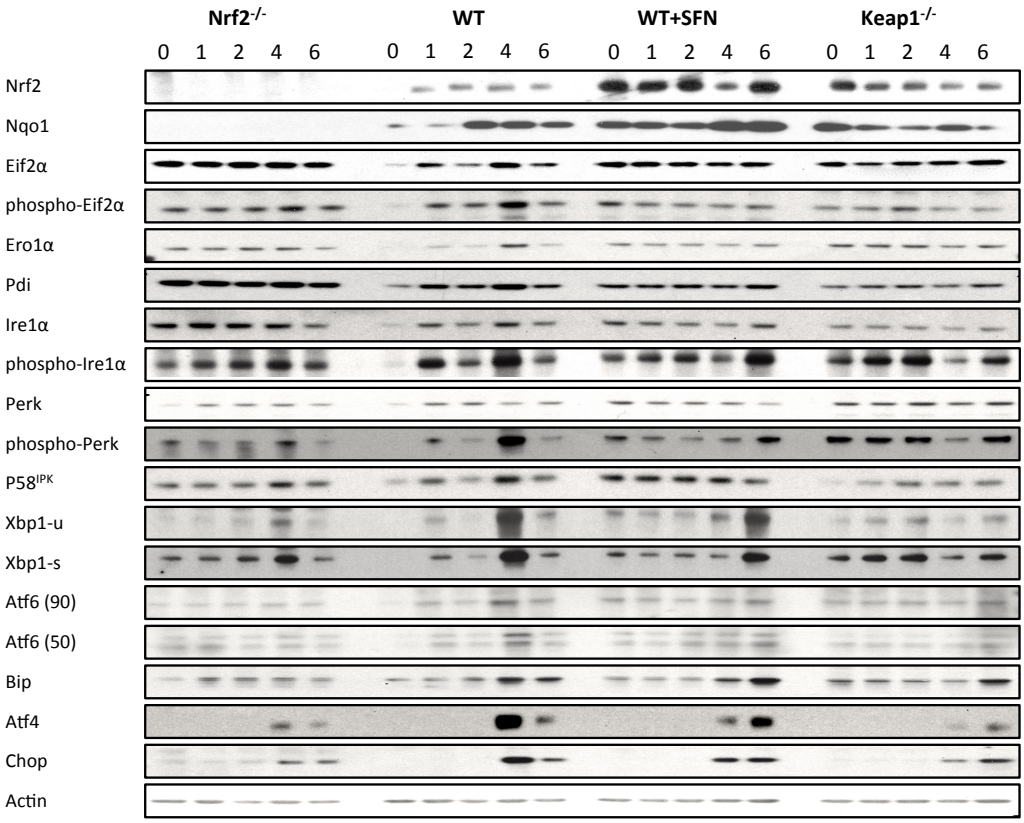

Figure 4.3 Western blot results of Experiment 3: Glucose starvation time course. ER stress response markers in MEF cells incubated in glucose-free DMEM for up to 6 hours. Key: WT= wild type; SFN = Sulforaphane.

4.2.5. Components of the UPR are differentially expressed in Keap1$^{-/-}$ cells under basal conditions

Western blotting results indicate that under basal conditions, Keap1$^{-/-}$ cells express increased protein levels of Perk and phospho-Perk, slightly increased Atf6 (90kDa) and reduced levels of Pdi and p58^{IPK}. However, despite increased basal phospho-Perk, protein levels of downstream effectors phospho-Eif2α, Atf4 and Chop were not increased at baseline in Keap1$^{-/-}$ cells. Taking into consideration the findings that Nrf2$^{-/-}$ cells had increased downstream effectors of the Perk arm of the UPR, these results provide further indication that Nrf2

modulates the activity of Perk, possibly with uninhibited Nrf2 repressing phospho-Perk kinase activity in a negative feedback cycle.

4.2.6 The response of Nrf2$^{-/-}$ MEFs, Keap1$^{-/-}$ MEFs and SFN treated WT cells to ER stress induction

4.2.6.1 WT cells

When subject to glucose starvation, components of the UPR were induced in a time-dependent manner and peaked at 4-6 hours regardless of cell type, demonstrated by expression levels of Atf4, Chop and Bip shown in Figure 4.3. In WT cells, expression of these components as well as phospho-Eif2α, phospho-Ire1α and spliced and unspliced forms of Xbp1, appear to peak at 4hours. (The lack of observable Chop expression in WT cells in Experiment 1 was suspected to be a false negative finding due to difficulties obtaining western blots for Chop in this experiment. This was confirmed following evident Chop induction in WT cells in further experiments.) Tm treatment also strongly induced the expression of Atf4, Chop and Bip in WT cells as well as other cell types.

4.2.6.2 Nrf2$^{-/-}$ cells

Expression of the downstream Perk signalling molecules Atf4 and Chop was induced in Nrf2$^{-/-}$ cells subject to ER stress induction. When cells were deprived of glucose this occurred notably at T=4hrs, but to a lesser extent than in WT counterparts at this time-point. Taken that these were seen to be increased at base-line; this finding could be explained by cells with constitutively increased Perk activity being less able to respond to ER stress. Bip was induced in Nrf2$^{-/-}$ cells, to a lesser extent than WT, by both glucose starvation and Tm challenge. In response to Tm challenge, Xbp1 protein expression in Nrf2$^{-/-}$ cells did not increase from basal levels but remained higher in Nrf2$^{-/-}$ than in WT cells following Tm. This could be explained if Xbp1 was already being maximally expressed. These results suggest that Nrf2$^{-/-}$ cells are less able to mount an effective, adaptive UPR response.

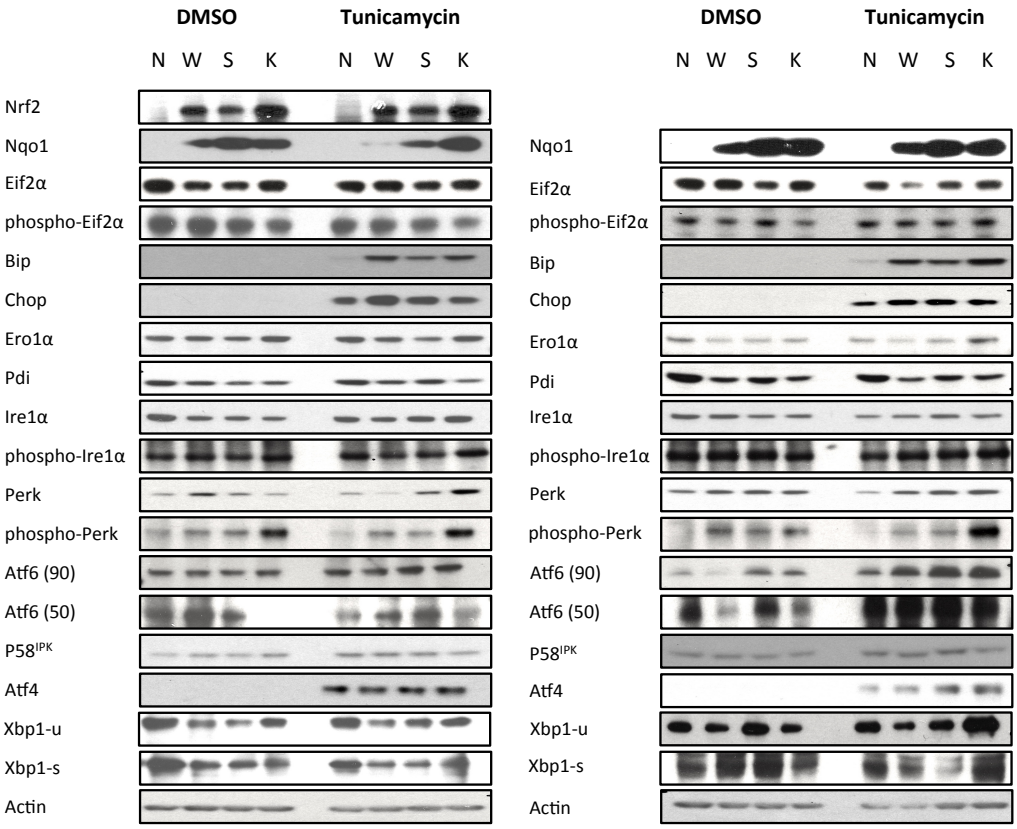

Figure 4.4 Western blot results of Experiment 4, performed in duplicate: ER stress response markers in MEF cells treated with Tunicamycin. Cells were treated with Tunicamycin or control (DMSO) for 6 hours. Key: N =Nrf2$^{-/-}$; W= wild type; S = WT + Sulforaphane; K=Keap1$^{-/-}$.

4.2.6.3 WT + SFN cells

Cells treated with SFN showed an increased expression of Eif2α throughout the glucose deprivation time-course compared to WT cells alone. The induction of UPR components in cells treated with SFN also appears to occur at a later time-point, at around 6 hours. This again provides evidence suggesting that increased Nrf2 activity in cells with SFN treatment modulates the activity of the Perk arm of the UPR. The response to Tm challenge in SFN treated cells was very similar and in keeping with the response of WT cells.

4.2.6.4 Keap1$^{-/-}$ cells

The general pattern of increased expression of UPR components such as Bip, phospho-Eif2α, Atf4 and Chop was also seen in Keap1$^{-/-}$ cells subject to ER stress. The induction of ER stress markers by glucose starvation was observed to

occur more strongly at the later time-point of 6hours in Keap1$^{-/-}$ cells, compared to 4hours in WT cells. Keap1$^{-/-}$ cells appear to have a more gradual response to glucose starvation, possibly peaking later than the time-course studied. This supports the hypothesis that cells with up-regulated Nrf2 might be less susceptible to ER stress. In response to Tm challenge, Xbp1, the 50kDa fragment of Atf6 were strongly induced in Keap1$^{-/-}$ cells compared to WT cells, demonstrating that the response to ER stress is altered in cells with increased Nrf2 activity, and also engages the Ire1a and Atf6 arms of the UPR.

4.2.7 Basal mRNA expression of ER stress markers in Nrf2$^{-/-}$ and Keap1$^{-/-}$ cells compared to WT

Results of q-rtPCR are demonstrated in Figures 4.5 to 4.7 (glucose deprivation) and Figures 4.8 to 4.10 (tunicamycin challenge). These results represent a set of triplicates for each sample from one experiment; therefore, error bars indicate experimental error and only limited conclusions may be inferred from these results.

4.2.7.1 Nrf2$^{-/-}$ cells

Consistently with protein expression, q-rtPCR of glucose deprivation showed significantly increased basal mRNA levels of total-Xbp1, Atf4 (both approximately 3 fold), Chop (10 fold), and Ero1α (10-15 fold) in Nrf2$^{-/-}$ cells compared to WT. However, increases in these genes did not reach significance in data from tunicamycin challenge, but instead demonstrated a trend towards increase.

4.2.7.2 Keap1$^{-/-}$ cells

Compared to WT, Keap1$^{-/-}$ cells demonstrated a trend of basal increase in mRNA levels of Ire1α, Eif2α, Chop, total-Xbp1 and spliced-Xbp1 (the latter two reaching significance in glucose starvation and Tm, respectively). These findings appear to contradict the protein expression data, however fold changes were not dramatically increased and it is also possible that mRNA is undergoing increased post-transcriptional or post-translational degradation. The lack of increased Perk mRNA expression may indicate that phospho-Perk protein accumulation in Keap1$^{-/-}$ cells is not related to upregulated expression.

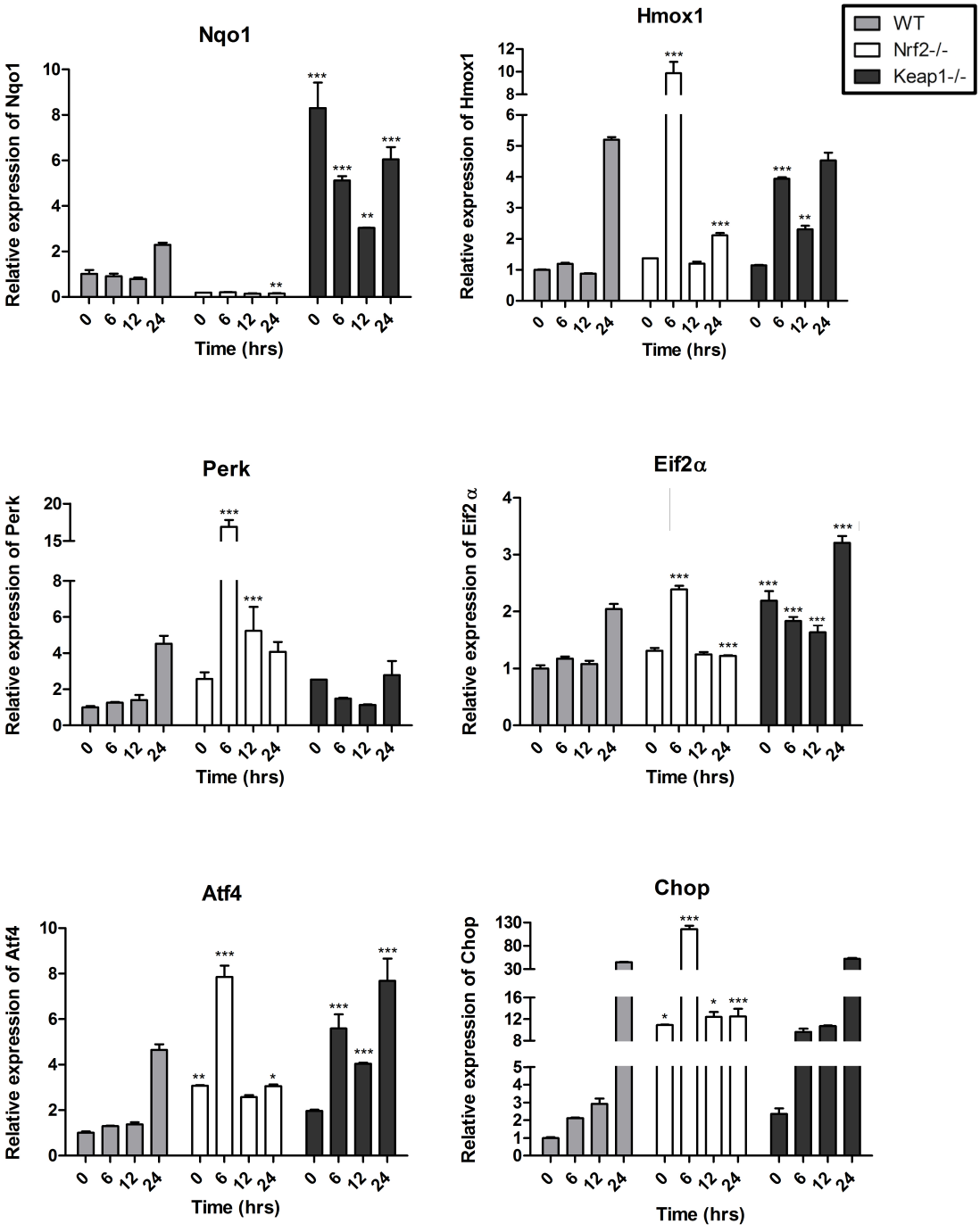

Figure 4.5 Glucose starvation time course rtPCR results: Relative mRNA expression of ER stress markers in MEF cells incubated in glucose-free DMEM for up to 24 hours. ER stress response markers in. Key: WT wild type; SFN = Sulforaphane. Data presented is from one experiment. Significance compared to corresponding WT time-point: *P ≤0.05; ** P ≤0.01; *** P ≤0.001.

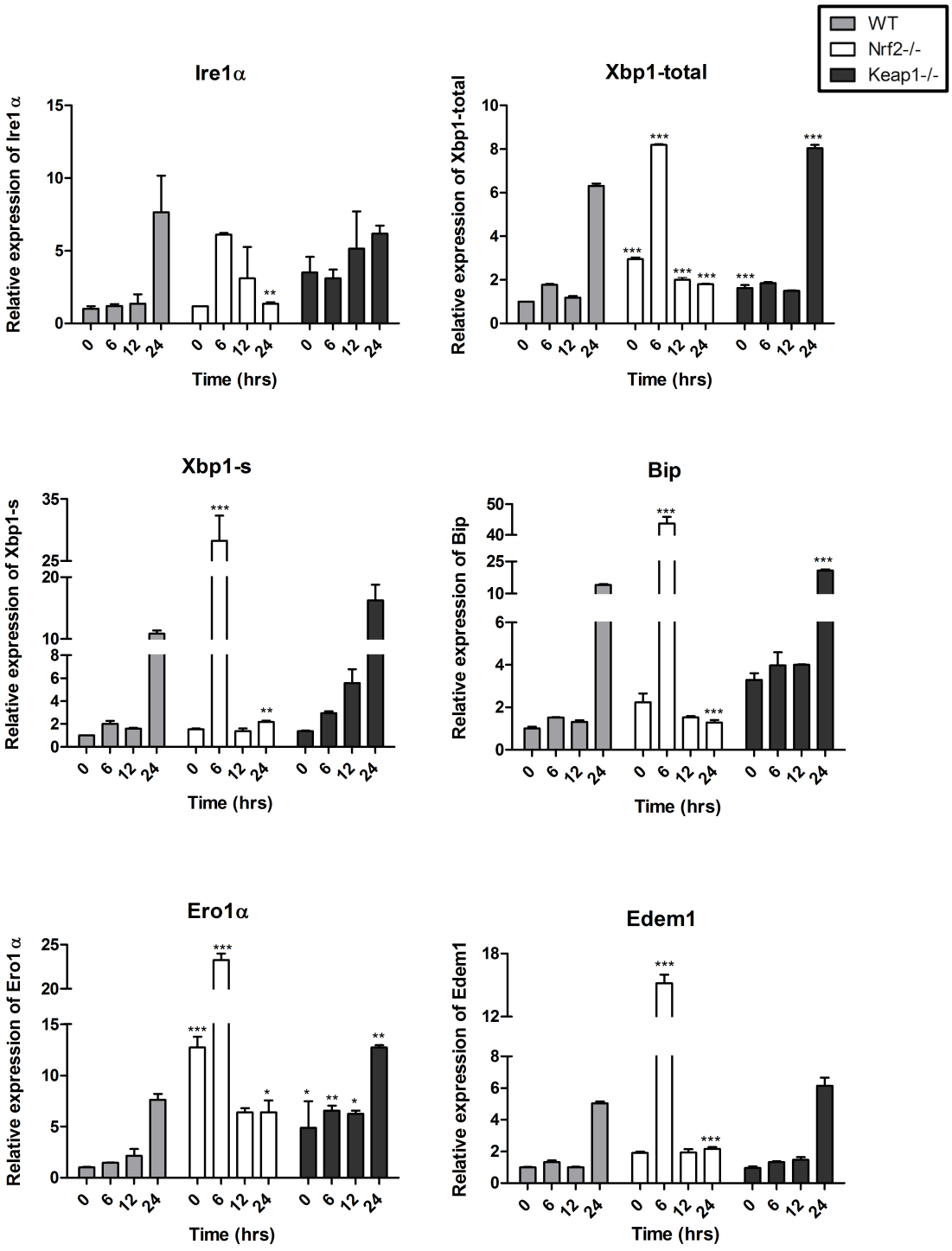

Figure 4.6 Glucose starvation time course rtPCR results: Relative mRNA expression of ER stress markers in MEF cells incubated in glucose-free DMEM for up to 24 hours. ER stress response markers in. Key: WT= wild type; SFN = Sulforaphane. Data presented is from one experiment. Significance compared to corresponding WT time-point: *P ≤0.05; ** P ≤0.01; *** P ≤0.001.

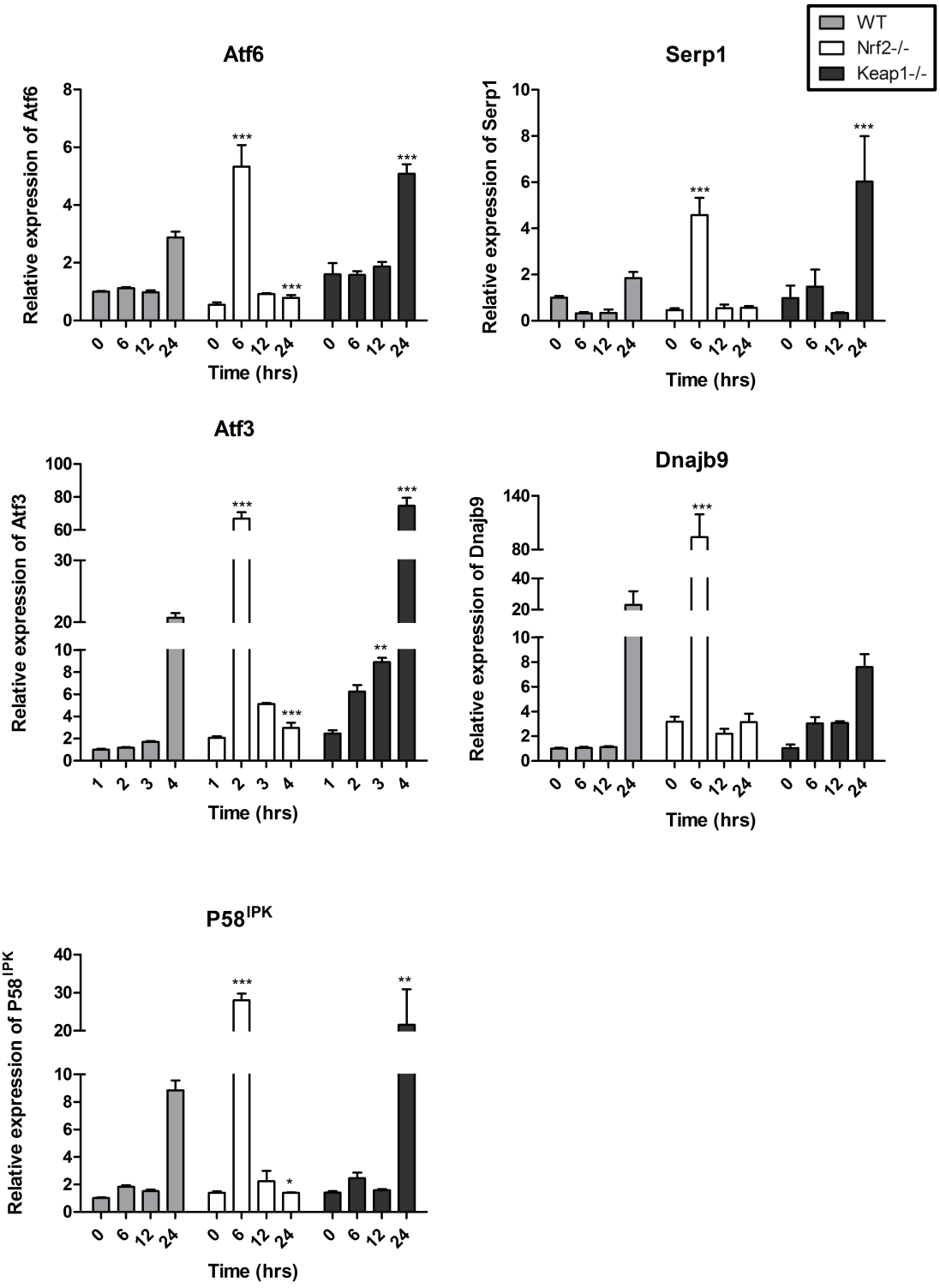

Figure 4.7 Glucose starvation time course rtPCR results: Relative mRNA expression of ER stress markers in MEF cells incubated in glucose-free DMEM for up to 24 hours. ER stress response markers in. Key: WT= wild type; SFN = Sulforaphane. Data presented is from one experiment. Significance compared to corresponding WT time-point: *P ≤0.05; ** P ≤0.01; *** P ≤0.001.

4.2.8 Gene expression in response to ER stress

Cells were stressed using methods of either glucose starvation or Tm treatment, and mRNA was collected over a 24hour time-course.

4.2.8.1 WT cells

When WT cells were subject to glucose deprivation, mRNA expression was induced for all of the ER stress markers investigated. These all followed a pattern of levels remaining at baseline or slightly increasing until 24hours, where a much larger, maximal induction occurred. The most notable increase in WT cells was in Chop mRNA, which was increased by over 50-fold at 24hours. When WT cells were stressed with Tm the pattern of induction followed a more time-dependent course, but again with maximal induction occurring at 24hours.

4.2.8.2 Nrf2$^{-/-}$ cells

In response to glucose starvation, almost all components of the UPR were significantly and dramatically induced in Nrf2$^{-/-}$ cells at 6hours, after which time these tapered down and many where reduced compared to WT at 24hours. This contrasts with the induction of many UPR components in WT and Keap1$^{-/-}$ cells, which typically peaked at 24hours. The 6-hour peak of UPR targets did not occur in Nrf2$^{-/-}$ cells when stress was induced by Tm. In this situation, the Nrf2$^{-/-}$ cells, similarly to WT and Keap1$^{-/-}$ cells, exhibited a time-dependent pattern of increasing in UPR induction with maximal response at 24hours. This could potentially mean that Nrf2$^{-/-}$ cells are more sensitive to glucose deprivation than other forms of ER stress, and this seems plausible, as Nrf2 regulates numerous targets, including genes involved in glucose homeostasis.

Interestingly, Nrf2$^{-/-}$ cells had increased levels of Perk mRNA compared to WT cells induced by ER stress regardless of method. This again strongly suggests that Nrf2 has some influence over the expression of Perk and the Perk UPR pathway.

4.2.8.3 Keap1$^{-/-}$ cells

Induction of mRNA expression in Keap1$^{-/-}$ cells followed very similar patterns to WT cells in both glucose deprivation and Tm time-courses. However, induction

of the UPR was to much greater extent in Keap1$^{-/-}$ cells at 24hours compared to WT cells.

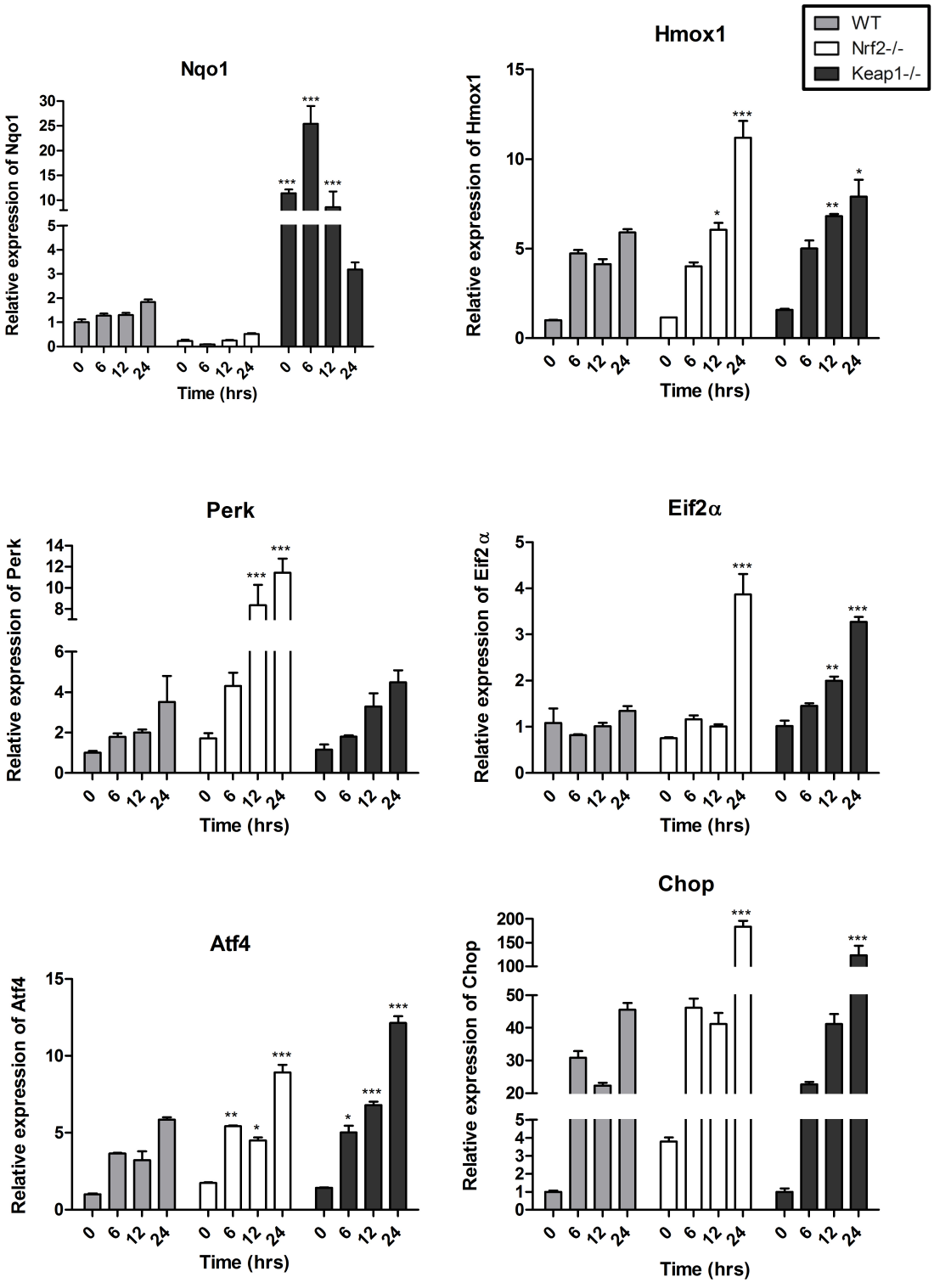

Figure 4.8 Tunicamycin treatment rtPCR results: mRNA expression ER stress response markers in MEF cells treated with Tunicamycin for up to 24hours. Cells were treated with Tunicamycin or control (DMSO) for 6 hours. Key: WT= wild type; SFN = Sulforaphane. Data presented is from one experiment. Significance compared to corresponding WT time-point: *P ≤0.05; ** P ≤0.01; *** P ≤0.001.

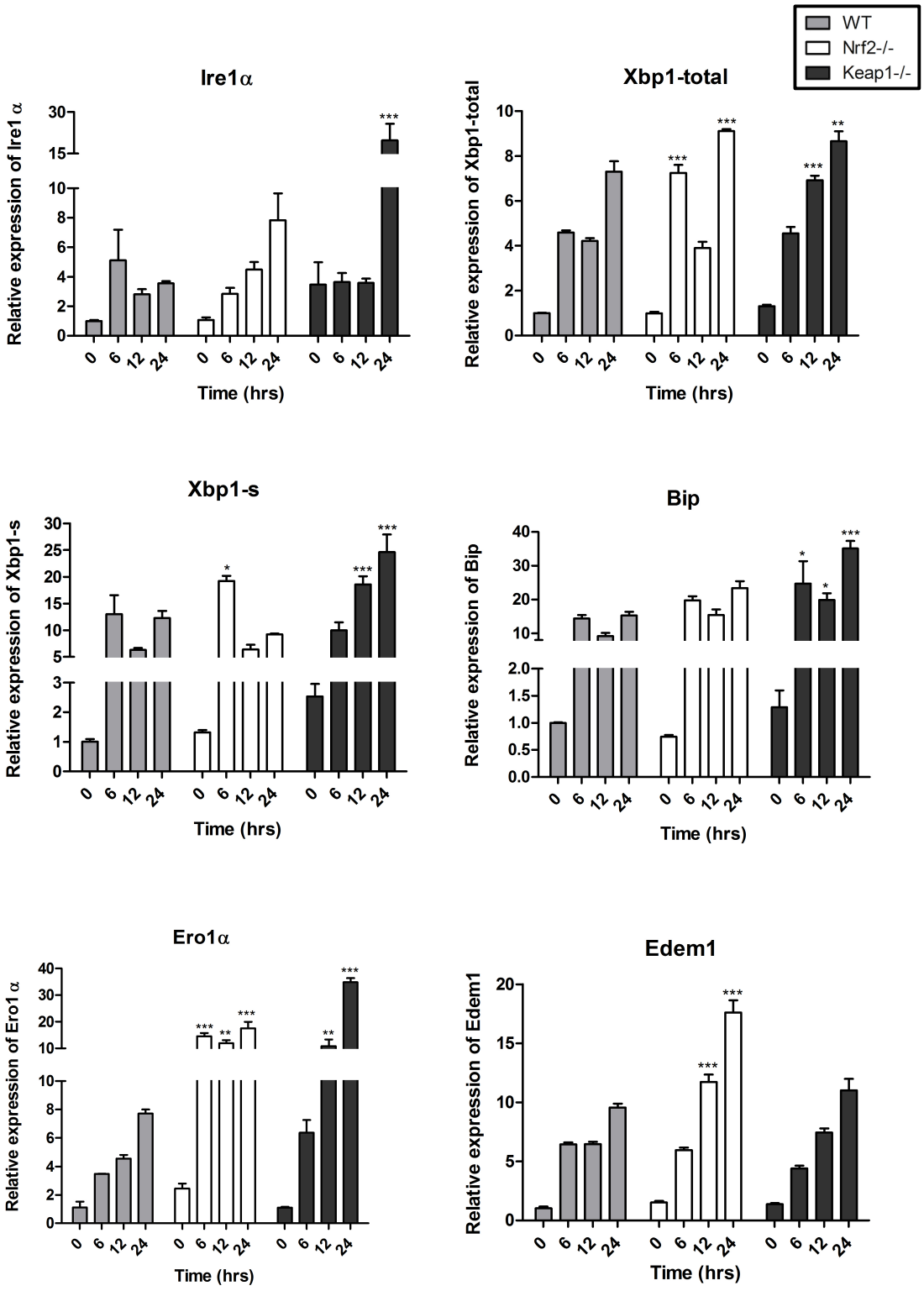

Figure 4.9 Tunicamycin treatment rtPCR results: mRNA expression ER stress response markers in MEF cells treated with Tunicamycin for up to 24hours. Cells were treated with Tunicamycin or control (DMSO) for 6 hours. Key: WT= wild type; SFN = Sulforaphane. Data presented is from one experiment. Significance compared to corresponding WT time-point: *P ≤0.05; ** P ≤0.01; *** P ≤0.001.

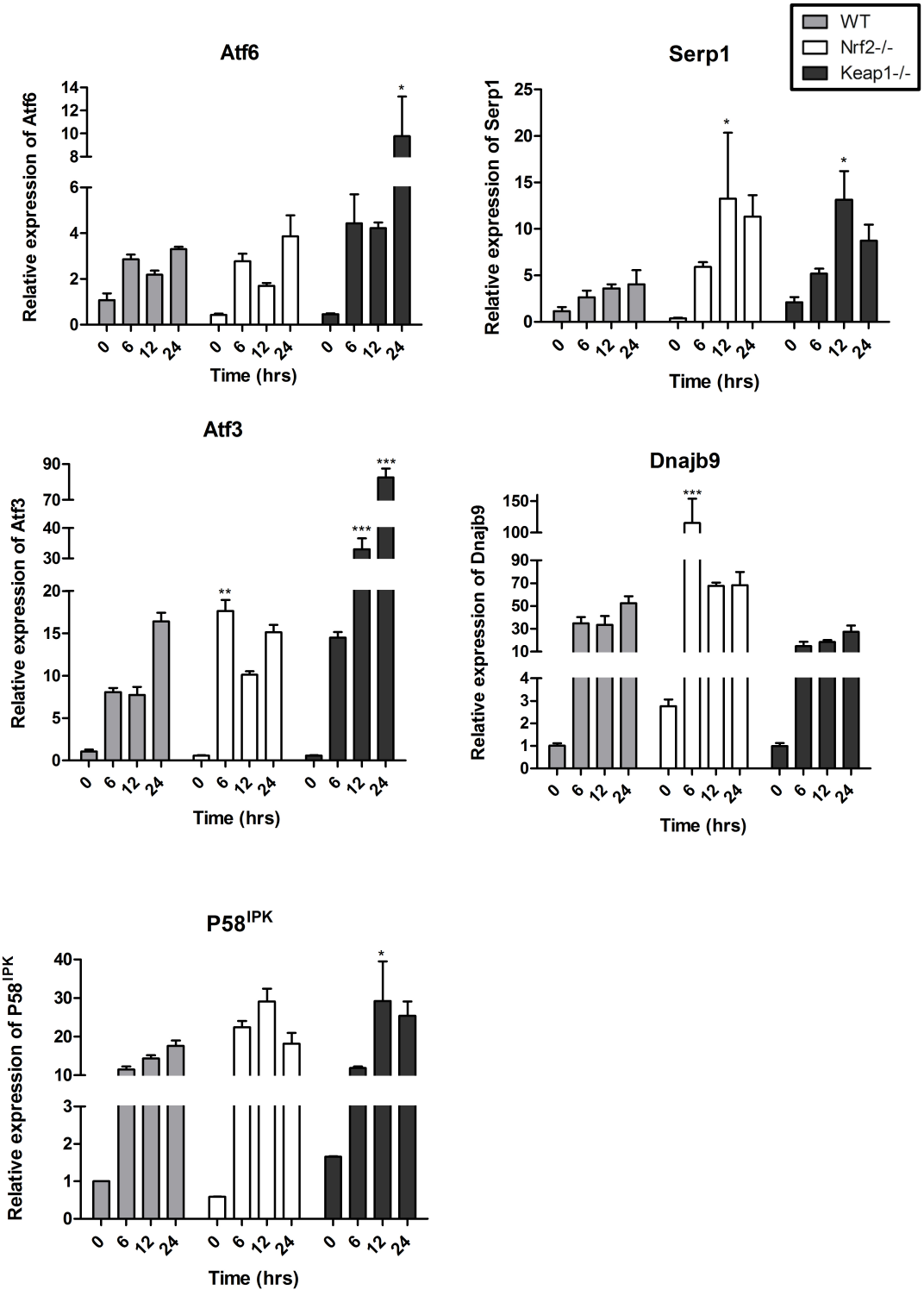

Figure 4.10 Tunicamycin treatment rtPCR results: mRNA expression ER stress response markers in MEF cells treated with Tunicamycin for up to 24hours. Cells were treated with Tunicamycin or control (DMSO) for 6 hours. Key: WT= wild type; SFN = Sulforaphane. Data presented is from one experiment. Significance compared to corresponding WT time-point: *P ≤0.05; ** P ≤0.01; *** P ≤0.001.

4.3 Discussion

Results herein demonstrate clear differences between cells under basal conditions, with a generalised increase in the expression of ER chaperone and UPR pathway proteins in $Nrf2^{-/-}$ cells compared to WT, providing evidence that $Nrf2^{-/-}$ cells may be subject to constitutive ER stress. The oxidoreductins Ero1α and Pdi were consistently basally upregulated in $Nrf2^{-/-}$ cells, indicative of homeostatic readjustment to alterations in the ER REDOX potential in the absence of Nrf2.

Basal protein levels of Perk and phospho-Perk were found to be increased in $Keap1^{-/-}$, but without increased downstream effects, compared to WT. Conversely, $Nrf2^{-/-}$ cells demonstrated increased levels of downstream effectors of Perk. These results strongly suggest that Nrf2 modulates the activity of Perk, with increased Nrf2 suppressing phospho-Perk kinase activity, possibly in a negative feedback cycle. Further supporting this, levels of $p58^{IPK}$, a co-chaperone protein that has an inhibitory effect of Perk, were reduced in $Keap1^{-/-}$.

The response to induced ER stress also varied with cellular Nrf2 status: The maximal expression of UPR components induced by glucose deprivation occurred at 4 hours in WT cells and in $Nrf2^{-/-}$ cells. Interestingly, the magnitude of the response was considerably smaller in $Nrf2^{-/-}$ cells. Taken together, it is suggested that because $Nrf2^{-/-}$ cells have basal ER stress, they have less ability to respond to conditions of increased stress. $Keap1^{-/-}$ cells were found to have a reduced response to glucose deprivation at 6hours, suggesting that longer conditions of ER stress are required to activate the UPR with increased availability of Nrf2.

These results clearly demonstrate that altered Nrf2 status affects the cellular response to ER stress. It is proposed that Nrf2 is involved in a negative feedback mechanism with the UPR pathways, whereby Nrf2 activity induced by UPR helps to alleviate ER stress, possibly by increasing glutathione and optimising the ER redox environment, and increased Nrf2 down-regulates the ER response. This would explain why $Nrf2^{-/-}$ cells express increased UPR proteins under basal conditions, due to a lack of negative feedback. With sustained increases in Nrf2,

such as in Keap1$^{-/-}$, cells have conferred resistance against ER stress; however, the balance of the UPR pathways becomes skewed towards the Perk arm. It is possible that Nrf2 has a role in the feedback mechanism by which cells are able to have different responses depending on the intensity and duration of ER stress, for example, sustained ER stress despite activation of Nrf2 may induce cells to go down the apoptotic pathway via Perk.

4.3.1 Relevance to other work in this field

Previous work has shown that the Nrf2/ARE pathway is induced under conditions of ER stress(84). Mechanistically, this could occur either in response to increased ROS during ER stress, via an interaction with signalling components of the UPR or as a combination of these. In similarity to our results, Cullinan and Diehl found that Nrf2$^{-/-}$ MEF cells were more sensitive to ER stress (85). Although they focused on the Perk arm of the UPR, and did not examine the other UPR markers, they found that Chop was basally increased in Nrf2$^{-/-}$ cells, in agreement with the rtPCR results of this project.

Cullinan and Diehl showed that in WT cells, glucose deprivation induced the nuclear translocation of Nrf2 and increased mRNA of Nrf2 targets Gclc and Nqo1 (85). This did not occur in Nrf2$^{-/-}$ cells, which displayed basally increased and consistently high levels of ROS and carbonyl-modified products, demonstrating oxidative stress. Whereas WT cells were transient increase in glutathione levels under conditions of glucose starvation, glutathione rapidly decreased in Nrf2$^{-/-}$ cells, providing evidence that Nrf2 participates in the cellular response to ROS during ER stress.

The study also demonstrated that Perk$^{-/-}$ cells were similarly unable to increase glutathione levels in response to increased ROS during ER stress, despite normal basal glutathione levels (85). Nuclear translocation of Nrf2 did not occur in response to ER stress in Perk$^{-/-}$ cells, and Nqo1 and Gclc were not induced (84). However, the addition of constitutively activated Nrf2 to Perk$^{-/-}$ cells was able to rescue Perk$^{-/-}$ cells. Similarly, *N*-acetyl-cysteine (NAC) has been shown to reduce apoptosis induced by ER stress in Nrf2$^{-/-}$ and Perk$^{-/-}$ cells (84, 85). Studies

in the same lab demonstrated that Nrf2 did not activate an ARE reporter in the presence of dominant-negative Perk and that overexpression of Perk promoted the nuclear translocation of Nrf2 in the absence of any ER stress inducing agent(84). These findings implicate Nrf2 as a target of the Perk arm of the UPR. $Perk^{-/-}$ cells were shown to have normal basal levels of ROS and Nrf2, leading the authors to suggest that the main contribution of Perk to REDOX homeostasis occurs under conditions of ER stress (68).

A study investigating the effects of chemotherapeutic alkylating agents has recently demonstrated an inter-relationship between Nrf2/ARE and ER stress pathways (35). Drugs of the alkylating agent class were shown to promote the nuclear accumulation of Nrf2, as well as ARE target gene induction and UPR components *in vitro*.

Alkylating agent related toxicity and caspase-3 induction were potentiated by Nrf2 silencing, but was supressed by both Keap1-knockdown or Nrf2 overexpression, providing evidence that Nrf2 activation confers a protective advantage against these agents. Supplementation of WT cells with the glutathione precursor substrates NAC or glutathione-ethyl-ester also reduced the toxicity of alkylating agents, whereas depletion of glutathione by the known inhibitor buthionine sulfoximine increased toxicity.

The study found that alkylating agents caused ER stress, demonstrated by increased Atf6 cleavage, expression of Ire1α, phosphorylation of Perk, and upregulation of UPR components; Bip, Atf3 and Chop. Inhibition of cell growth and caspase-3 induction due to alkylating agents were supressed by Perk silencing but potentiated by reduction of either Atf6 or Ire1α. Bip overexpression was also shown to attenuate cytotoxicity. The study showed that nuclear accumulation of Nrf2, ARE induction and glutathione biosynthesis did not require either Perk, Ire1α or Atf6, demonstrating that in this context, Nrf2 activation was not a downstream component of the UPR. Instead, Nrf2 depletion was found to increase the expression of ER stress markers and potentiate UPR induction. Pre-treatment with NAC was found to attenuate the expression of

UPR components in WT cells, but was also able to attenuate increases in ER stress in Nrf2 depleted cells.

These findings support the results herein that loss of Nrf2 activity makes cells more susceptible to ER stress. These findings also suggest that Nrf2 mediated glutathione biosynthesis is an important factor in attenuation of alkylating agent induced ER stress and cytotoxicity.

4.3.2 Further work

This study has utilised Tm treatment and glucose starvation techniques to induce ER stress. Interplay between Nrf2 and components of the UPR could be further assessed using additional methods for inducing ER stress. There are further pharmacological agents known to induce ER stress, for example, treatment with thapsigargin induces ER stress by inhibition of the ER Ca^{2+}-ATPase, an ER transporter that is important for many Ca^{2+} dependent ER chaperones (83, 86).

As described in Chapter 1, NAFLD is strongly associated with perturbed lipid homeostasis and hyperglycaemia. Saturated fatty acids are known to induce ER stress in vitro and in vivo, and hyperglycaemia has also been shown to cause ER stress and both induce UPR and inflammatory pathways (68, 74-77, 87-90). Further work to determine the role of Nrf2 in the context of ER stress induced by saturated fatty acids or hyperglycaemia may be of particular importance to understanding the pathogenesis of NAFLD.

4.4 Conclusion

The pathogenesis of NASH is not fully understood, but is thought to involve interacting mechanisms of damage, whereby insulin resistance and hepatic storage of triacylglycerides (resulting in steatosis) is compounded by further cellular insult leading to inflammation and fibrosis. ER stress activates pathways of the unfolded protein response (UPR), which act to attenuate stress, adapt to conditions and achieve ER homeostasis. However, if the cell is unable restore normal ER functioning under conditions of chronic ER stress, the sustained UPR interacts with other cell signalling pathways to drive the cell to apoptosis. Both oxidative stress and ER stress are known to contribute to many diseases and the

role of cellular stress in liver disease has been a subject of much interest in recent years. Cross talk between these stress response pathways is likely, and in this project the role of Nrf2 in ER stress has been investigated. The UPR may have particular importance in NASH as the ER is involved in the regulation of metabolism and inflammation and protein synthesis is a major role of hepatocytes.

Bibliography

1. Bertot LC, Adams LA. The natural course of non-alcoholic fatty liver disease. Int J Mol Sci. 2016;17(5):774.
2. Ludwig J, McGill DB, Lindor KD. Review: nonalcoholic steatohepatitis. J Gastroenterol Hepatol. 1997;12(5):398-403.
3. Ludwig J, Viggiano TR, McGill DB, Oh BJ. Nonalcoholic steatohepatitis: Mayo Clinic experiences with a hitherto unnamed disease. Mayo Clin Proc. 1980;55(7):434-8.
4. Fuchs M, Sanyal AJ. Lipotoxicity in NASH. J Hepatol. 2012;56(1):291-3.
5. Vernon G, Baranova A, Younossi ZM. Systematic review: The epidemiology and natural history of non-alcoholic fatty liver disease and non-alcoholic steatohepatitis in adults. Aliment Pharm Therap. 2011;34:274-85.
6. Lim JS, Mietus-Snyder M, Valente A, Schwarz JM, Lustig RH. The role of fructose in the pathogenesis of NAFLD and the metabolic syndrome. Nat Rev Gastroenterol Hepatol. 2010;7(5):251-64.
7. Younossi ZM, Koenig AB, Abdelatif D, Fazel Y, Henry L, Wymer M. Global Epidemiology of Non-Alcoholic Fatty Liver Disease-Meta-Analytic Assessment of Prevalence, Incidence and Outcomes. Hepatology. 2015;64(1):73-84.
8. Glen J, Floros L, Day C, Pryke R. Non-alcoholic fatty liver disease (NAFLD): summary of NICE guidance. BMJ. 2016;354:i4428-i.
9. Brunt EM, Wong VWS, Nobili V, Day CP, Sookoian S, Maher JJ, et al. Nonalcoholic fatty liver disease. Nat Rev Dis Prim. 2015(December):15080.
10. Brunt EM, Kleiner DE, Wilson LA, Belt P, Neuschwander-Tetri BA, Network NCR. Nonalcoholic fatty liver disease (NAFLD) activity score and the histopathologic diagnosis in NAFLD: distinct clinicopathologic meanings. Hepatology. 2011;53(3):810-20.
11. Rinella ME, Sanyal AJ. Management of NAFLD: a stage-based approach. Nat Rev Gastroenterol Hepatol. 2016;13(4):196-205.
12. Hardy T, Anstee QM, Day CP. Non-alcoholic fatty liver disease: new treatments. Curr Opin Gastroenterol. 2015;31:175-83.
13. Neuschwander-Tetri BA, Loomba R, Sanyal AJ, Lavine JE, Van Natta ML, Abdelmalek MF, et al. Farnesoid X nuclear receptor ligand obeticholic acid for non-cirrhotic, non-alcoholic steatohepatitis (FLINT): a multicentre, randomised, placebo-controlled trial. Lancet. 2015;385(9972):956-65.
14. Duwaerts CC, Maher JJ. Mechanisms of liver injury in non-alcoholic steatohepatitis. Curr Hep Rep. 2014;13(2):119-29.
15. Tiniakos DG, Vos MB, Brunt EM. Nonalcoholic Fatty Liver Disease: Pathology and Pathogenesis. Annu Rev Pathol. 2010;5(1):145-71.
16. Day CP. NASH-related liver failure: One hit too many? Am J Gastroenterol. 2002;97(8):1872-4.
17. Tilg H, Moschen AR, Roden M. NAFLD and diabetes mellitus. Nat Rev Gastroenterol Hepatol. 2016;14(1):32-42.
18. Nguyen P, Leray V, Diez M, Serisier S, Le Bloc'h J, Siliart B, et al. Liver lipid metabolism. J Anim Physiol Anim Nutr. 2008;92(3):272-83.
19. Mello T, Materozzi M, Galli A. PPARs and Mitochondrial Metabolism: From NAFLD to HCC. PPAR Res. 2016;ID: 7403230.

20. Horton JD, Goldstein JL, Brown MS. SREBPs: activators of the complete program of cholesterol and fatty acid synthesis in the liver. J Clin Invest. 2002;109(9):1125-31.
21. Michalik L, Auwerx J, Berger JP, Chatterjee VK, Glass CK, Gonzalez FJ, et al. International Union of Pharmacology. LXI. Peroxisome proliferator-activated receptors. Pharmacol Rev. 2006;58(4):726-41.
22. Preidis GA, Kim KH, Moore DD. Nutrient-sensing nuclear receptors PPARalpha and FXR control liver energy balance. J Clin Invest. 2017;127(4):1193-201.
23. Schieber M, Chandel NS. ROS Function in Redox Signaling and Oxidative Stress. Curr Biol. 2014;24(10):R453-R62.
24. Lushchak VI, Lushchak VI. Glutathione Homeostasis and Functions: Potential Targets for Medical Interventions. J Amino Acids. 2012:1-26.
25. Zhang H, Davies KJA, Forman HJ. Oxidative stress response and Nrf2 signaling in aging. Free Radic Biol Med. 2015;88(Part B):314-36.
26. Mimura J, Itoh K. Role of Nrf2 in the pathogenesis of atherosclerosis. Free Radic Biol Med. 2015;88(Part B):221-32.
27. Tebay LE, Robertson H, Durant ST, Vitale SR, Penning TM, Dinkova-Kostova AT, et al. Mechanisms of activation of the transcription factor Nrf2 by redox stressors, nutrient cues, and energy status and the pathways through which it attenuates degenerative disease. Free Radic Biol Med. 2015;88(Part B):108-46.
28. Rushmore TH, King RG, Paulson KE, Pickett CB. Regulation of glutathione S-transferase Ya subunit gene expression: identification of a unique xenobiotic-responsive element controlling inducible expression by planar aromatic compounds. P Natl Acad Sci USA. 1990;87(10):3826-30.
29. Rushmore TH, Morton MR, Pickett CB. The antioxidant responsive element: Activation by oxidative stress and identification of the DNA consensus sequence required for functional activity. J Biol Chem. 1991;266(18):11632-9.
30. Rushmore TH, Pickett CB. Transcriptional regulation of the rat glutathione S-transferase Ya subunit gene. Characterization of a xenobiotic-responsive element controlling inducible expression by phenolic antioxidants. J Biol Chem. 1990;265(24):14648-53.
31. Itoh K, Chiba T, Takahashi S, Ishii T, Igarashi K, Katoh Y, et al. An Nrf2/Small Maf Heterodimer Mediates the Induction of Phase II Detoxifying Enzyme Genes through Antioxidant Response Elements. Biochem Bioph Res Co. 1997;236(2):313-22.
32. Tong KI, Katoh Y, Kusunoki H, Itoh K, Tanaka T, Yamamoto M, et al. Keap1 Recruits Neh2 through Binding to ETGE and DLG Motifs: Characterization of the Two-Site Molecular Recognition Model. Mol Cell Biol. 2006;26(8):2887-900.
33. Tong KI, Kobayashi A, Katsuoka F, Yamamoto M. Two-site substrate recognition model for the Keap1-Nrf2 system: A hinge and latch mechanism. Biol Chem. 2006;387(10-11):1311-20.
34. Rada P, Rojo AI, Chowdhry S, McMahon M, Hayes JD, Cuadrado A. SCF/{beta}-TrCP promotes glycogen synthase kinase 3-dependent degradation of the Nrf2 transcription factor in a Keap1-independent manner. Mol Cell Biol. 2011;31(6):1121-33.
35. Zanotto-Filho A, Masamsetti VP, Loranc E, Tonapi SS, Gorthi A, Bernard X, et al. Alkylating Agent-Induced NRF2 Blocks Endoplasmic

Reticulum Stress-Mediated Apoptosis via Control of Glutathione Pools and Protein Thiol Homeostasis. Mol Cancer Ther. 2016;15(12):3000-14.
36. Meakin PJ, Chowdhry S, Sharma RS, Ashford FB, Walsh SV, McCrimmon RJ, et al. Susceptibility of Nrf2-null mice to steatohepatitis and cirrhosis upon consumption of a high-fat diet is associated with oxidative stress, perturbation of the unfolded protein response, and disturbance in the expression of metabolic enzymes but not with insulin resistance. Mol Cell Biol. 2014;34(17):3305-20.
37. Chowdhry S, Nazmy MH, Meakin PJ, Dinkova-Kostova AT, Walsh SV, Tsujita T, et al. Loss of Nrf2 markedly exacerbates nonalcoholic steatohepatitis. Free Radical Bio Med. 2010;48(2):357-71.
38. Hardwick RN, Fisher CD, Canet MJ, Lake AD, Cherrington NJ. Diversity in antioxidant response enzymes in progressive stages of human nonalcoholic fatty liver disease. Drug Metab Dispos. 2010;38(12):2293-301.
39. Voeltz GK, Rolls MM, Rapoport TA. Structural organization of the endoplasmic reticulum. EMBO Rep. 2002;3(10):944-50.
40. Fagone P, Jackowski S. Membrane phospholipid synthesis and endoplasmic reticulum function. J Lipid Res. 2009;50 Suppl:S311-6.
41. Hetz C. The unfolded protein response: controlling cell fate decisions under ER stress and beyond. Nat Rev Mol Cell Biol. 2012;13(2):89-102.
42. Pincus D, Chevalier MW, Aragon T, van Anken E, Vidal SE, El-Samad H, et al. BiP binding to the ER-stress sensor Ire1 tunes the homeostatic behavior of the unfolded protein response. PLoS Biol. 2010;8(7):e1000415.
43. Gardner BM, Pincus D, Gotthardt K, Gallagher CM, Walter P. Endoplasmic reticulum stress sensing in the unfolded protein response. Cold Spring Harb Perspect Biol. 2013;5(3):1-15.
44. Ozcan L, Tabas I. Role of Endoplasmic Reticulum Stress in Metabolic Disease and Other Disorders. Annu Rev Med. 2012;63:317-28.
45. Schroder M, Kaufman RJ. ER stress and the unfolded protein response. Mutat Res. 2005;569:29-63.
46. Cao SS, Kaufman RJ. Unfolded protein response. Curr Biol. 2012;22(16):622-6.
47. Pagliassotti MJ. Endoplasmic reticulum stress in nonalcoholic fatty liver disease. Annu Rev Nutr. 2012;32:17-33.
48. Nikawa J, Yamashita S. IRE1 encodes a putative protein kinase containing a membrane-spanning domain and is required for inositol phototrophy in Saccharomyces cerevisiae. Mol Microbiol. 1992;6(11):1441-6.
49. Cox JS, Shamu CE, Walter P. Transcriptional induction of genes encoding endoplasmic reticulum resident proteins requires a transmembrane protein kinase. Cell. 1993;73(6):1197-206.
50. Tirasophon W, Welihinda AA, Kaufman RJ. A stress response pathway from the endoplasmic reticulum to the nucleus requires a novel bifunctional protein kinase/endoribonuclease (Ire1p) in mammalian cells. Genes Dev. 1998;12(12):1812-24.
51. Credle JJ, Finer-Moore JS, Papa FR, Stroud RM, Walter P. On the mechanism of sensing unfolded protein in the endoplasmic reticulum. P Natl Acad Sci USA. 2005;102(52):18773-84.
52. Gardner BM, Walter P. Unfolded proteins are Ire1-activating ligands that directly induce the unfolded protein response. Science. 2011;333(6051):1891-4.

53. Lee K, Tirasophon W, Shen X, Michalak M, Prywes R, Okada T, et al. IRE1-mediated unconventional mRNA splicing and S2P-mediated ATF6 cleavage merge to regulate XBP1 in signaling the unfolded protein response. Genes Dev. 2002;16(4):452-66.
54. Shamu CE, Walter P. Oligomerization and phosphorylation of the Ire1p kinase during intracellular signaling from the endoplasmic reticulum to the nucleus. EMBO J. 1996;15(12):3028-39.
55. Sidrauski C, Walter P. The transmembrane kinase Ire1p is a site-specific endonuclease that initiates mRNA splicing in the unfolded protein response. Cell. 1997;90(6):1031-9.
56. Cox JS, Walter P. A novel mechanism for regulating activity of a transcription factor that controls the unfolded protein response. Cell. 1996;87(3):391-404.
57. Gonzalez TN, Sidrauski C, Dorfler S, Walter P. Mechanism of non-spliceosomal mRNA splicing in the unfolded protein response pathway. EMBO J. 1999;18(11):3119-32.
58. Lee AH, Iwakoshi NN, Glimcher LH. XBP-1 regulates a subset of endoplasmic reticulum resident chaperone genes in the unfolded protein response. Mol Cell Biol. 2003;23(21):7448-59.
59. Hollien J, Lin JH, Li H, Stevens N, Walter P, Weissman JS. Regulated Ire1-dependent decay of messenger RNAs in mammalian cells. J Cell Biol. 2009;186(3):323-31.
60. Reimold AM, Etkin A, Clauss I, Perkins A, Friend DS, Zhang J, et al. An essential role in liver development for transcription factor XBP-1. Genes Dev. 2000;14(2):152-7.
61. Piperi C, Adamopoulos C, Papavassiliou AG. XBP1: A Pivotal Transcriptional Regulator of Glucose and Lipid Metabolism. Trends Endocrinol Metab. 2016;27(3):119-22.
62. Ito D, Walker JR, Thompson CS, Moroz I, Lin W, Veselits ML, et al. Characterization of stanniocalcin 2, a novel target of the mammalian unfolded protein response with cytoprotective properties. Mol Cell Biol. 2004;24(21):9456-69.
63. Haze K, Yoshida H, Yanagi H, Yura T, Mori K. Mammalian transcription factor ATF6 is synthesized as a transmembrane protein and activated by proteolysis in response to endoplasmic reticulum stress. Mol Biol Cell. 1999;10(11):3787-99.
64. Ye J, Rawson RB, Komuro R, Chen X, Dave UP, Prywes R, et al. ER stress induces cleavage of membrane-bound ATF6 by the same proteases that process SREBPs. Mol Cell. 2000;6(6):1355-64.
65. Lin JH, Li H, Zhang Y, Ron D, Walter P. Divergent effects of PERK and IRE1 signaling on cell viability. PLoS One. 2009;4(1):e4170.
66. Urano F, Wang X, Bertolotti A, Zhang Y, Chung P, Harding HP, et al. Coupling of stress in the ER to activation of JNK protein kinases by transmembrane protein kinase IRE1. Science. 2000;287(5453):664-6.
67. Plate L, Cooley CB, Chen JJ, Paxman RJ, Gallagher CM, Madoux F, et al. Small molecule proteostasis regulators that reprogram the ER to reduce extracellular protein aggregation. Elife. 2016;5.
68. Mooradian AD, Haas MJ. Glucose-induced endoplasmic reticulum stress is independent of oxidative stress: A mechanistic explanation for the failure of antioxidant therapy in diabetes. Free Radic Biol Med. 2011;50(9):1140-3.

69. Back SH, Kaufman RJ. Endoplasmic reticulum stress and type 2 diabetes. Annu Rev Biochem. 2012;81:767-93.
70. Lake AD, Novak P, Hardwick RN, Flores-Keown B, Zhao F, Klimecki WT, et al. The Adaptive endoplasmic reticulum stress response to lipotoxicity in progressive human nonalcoholic fatty liver disease. Toxicol Sci. 2014;137(1):26-35.
71. Puri P, Mirshahi F, Cheung O, Natarajan R, Maher JW, Kellum JM, et al. Activation and Dysregulation of the Unfolded Protein Response in Nonalcoholic Fatty Liver Disease. Gastroenterology. 2008;134(2):568-76.
72. Expert Panel on Detection E, Treatment of High Blood Cholesterol in A. Executive Summary of The Third Report of The National Cholesterol Education Program (NCEP) Expert Panel on Detection, Evaluation, And Treatment of High Blood Cholesterol In Adults (Adult Treatment Panel III). JAMA. 2001;285(19):2486-97.
73. Kyrylkova K, Kyryachenko S, Leid M, Kioussi C. Detection of apoptosis by TUNEL assay. Methods Mol Biol. 2012;887:41-7.
74. Wang D, Wei Y, Pagliassotti MJ. Saturated fatty acids promote endoplasmic reticulum stress and liver injury in rats with hepatic steatosis. Endocrinology. 2006;147(2):943-51.
75. Wei Y, Wang D, Topczewski F, Pagliassotti MJ. Saturated fatty acids induce endoplasmic reticulum stress and apoptosis independently of ceramide in liver cells. Am J Physiol-Endoc M. 2006;291:275-81.
76. Haffar T, Bérubé-Simard F-A, Tardif J-C, Bousette N. Saturated fatty acids induce endoplasmic reticulum stress in primary cardiomyocytes. Endoplasmic Reticulum Stress in Diseases. 2015;2(1):53-66.
77. Jo H, Choe SS, Shin KC, Jang H, Lee JH, Seong JK, et al. Endoplasmic reticulum stress induces hepatic steatosis via increased expression of the hepatic very low-density lipoprotein receptor. Hepatology. 2013;57(4):1366-77.
78. Rutkowski DT, Wu J, Back SH, Callaghan MU, Ferris SP, Iqbal J, et al. UPR Pathways Combine to Prevent Hepatic Steatosis Caused by ER Stress-Mediated Suppression of Transcriptional Master Regulators. Dev Cell. 2008;15(6):829-40.
79. Dinkova-Kostova AT, Talalay P, Sharkey J, Zhang Y, Holtzclaw WD, Wang XJ, et al. An exceptionally potent inducer of cytoprotective enzymes: elucidation of the structural features that determine inducer potency and reactivity with Keap1. J Biol Chem. 2010;285(44):33747-55.
80. Wei E, Ben Ali Y, Lyon J, Wang H, Nelson R, Dolinsky VW, et al. Loss of TGH/Ces3 in mice decreases blood lipids, improves glucose tolerance, and increases energy expenditure. Cell Metab. 2010;11(3):183-93.
81. Stanton MC, Chen SC, Jackson JV, Rojas-Triana A, Kinsley D, Cui L, et al. Inflammatory Signals shift from adipose to liver during high fat feeding and influence the development of steatohepatitis in mice. J Inflamm. 2011;8:8.
82. Dinkova-Kostova AT, Holtzclaw WD, Cole RN, Itoh K, Wakabayashi N, Katoh Y, et al. Direct evidence that sulfhydryl groups of Keap1 are the sensors regulating induction of phase 2 enzymes that protect against carcinogens and oxidants. Proc Natl Acad Sci U S A. 2002;99(18):11908-13.
83. Oslowski CM, Urano F. Measuring ER stress and the unfolded protein response using mammalian tissue culture system. Methods in Enzymology. 2013(508):71-92.

84. Cullinan SB, Zhang D, Hannink M, Arvisais E, Kaufman RJ, Diehl JA. Nrf2 is a direct PERK substrate and effector of PERK-dependent cell survival. Mol Cell Biol. 2003;23(20):7198-209.
85. Cullinan SB, Diehl JA. PERK-dependent activation of Nrf2 contributes to redox homeostasis and cell survival following endoplasmic reticulum stress. J Biol Chem. 2004;279(19):20108-17.
86. Samali A, FitzGerald U, Deegan S, Gupta S. Methods for Monitoring Endoplasmic Reticulum Stress and the Unfolded Protein Response. Int J Cell B. 2010;2010:1-11.
87. Fiorentino TV, Procopio T, Mancuso E, Arcidiacono GP, Andreozzi F, Arturi F, et al. SRT1720 counteracts glucosamine-induced endoplasmic reticulum stress and endothelial dysfunction. Cardiovasc Res. 2015;107(2):295-306.
88. Back SH, Kang S-W, Han J, Chung H-T. Endoplasmic Reticulum Stress in the β-Cell Pathogenesis of Type 2 Diabetes. Exp Diabetes Res. 2012;2012(ID:618396):1-11.
89. Cui W, Ma J, Wang X, Yang W, Zhang J, Ji Q. Free fatty acid induces endoplasmic reticulum stress and apoptosis of beta-cells by Ca2+/calpain-2 pathways. PLoS One. 2013;8(3):e59921.
90. Sheikh-Ali M, Sultan S, Alamir A-R, Haas MJ, Mooradian AD. Hyperglycemia-induced endoplasmic reticulum stress in endothelial cells. Nutrition. 2010;26(11-12):1146-50.